Open orbits in Copper Fermi surface

Masatsugu Sei Suzuki and Itsuko S. Suzuki
Department of Physics, State University of New York at Binghamton
(Date: December 20, 2017)

David Shoenberg, MBE FRS, (4 January 1911 – 10 March 2004) was a British physicist. David Shoenberg was born in 1911, the son of Isaac Shoenberg. Isaac came to Britain and acquired British nationality, but then returned to Russia where David was born. David was, however, a British citizen, and was brought to Britain as a boy. He was educated at Latymer Upper School, Hammersmith and Trinity College, Cambridge, where he took his doctorate in 1935.

He began his research into aspects of low-temperature physics and magnetism at the Mond Laboratory at Cambridge. After the war he played a leading role in re-establishing low-temperature physics at Cambridge, becoming head of the Mond Laboratory in 1947. He remained in this post until 1973. He was Professor of Physics, Cambridge University and Head of Low Temperature Physics Group, Cavendish Laboratory, 1973–78, then Professor Emeritus. He was also a Life Fellow of Gonville and Caius College, Cambridge. He received the MBE in 1944. He was elected a Fellow of the Royal Society in 1953 and was awarded their Hughes Medal in 1995 "for his work on the electronic structure of solids, in particular by exploiting low temperature techniques, particularly the de Haas van Alphen effect".

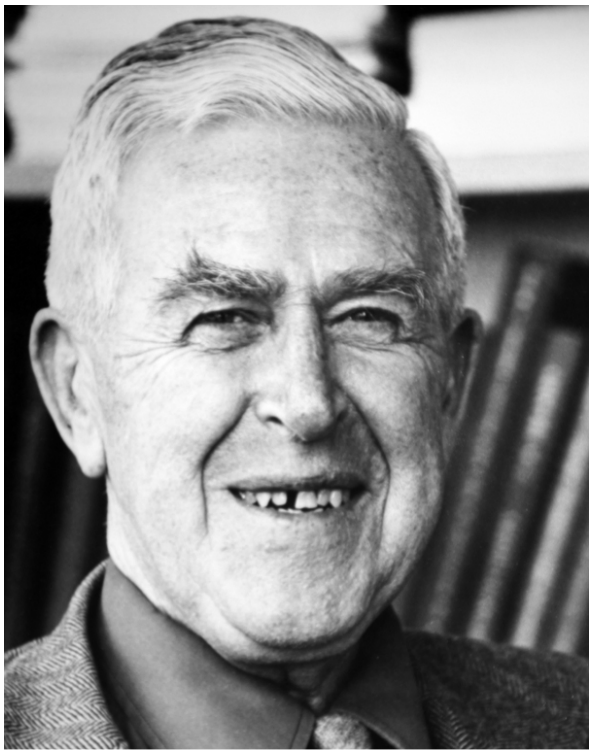

https://en.wikipedia.org/wiki/David_Shoenberg

1. My experience in doing de Haas-van Alphen effect

In order to get a nice signal of de Haas van Alphen (dHvA) effect in copper (Cu), we need a high quality of Cu sample (single crystal). We also need a strong magnetic field by using a superconducting magnet (5 tesla). The period of the dHvA oscillation is about 4 Oe for the belly orbit for the <100> direction. So the stability of the magnetic field is very important to get the good result. The experiment can be done at very low temperatures (liquid He temperatures). In 1974, I was a graduate student in the University of Tokyo. As a graduate student (the first year), I just started a sort of my research for doing experiment of de Haas van Alphen effect using copper as a part of training in the experimental physics.. The level of research in this field in Japan is much lower than that of Shoenberg and Pippard in Great Britain. My professor (Prof. Sei-ichi Tanuma) just wanted to know the quality of single crystal copper samples and the resolution of magnetic field of the superconducting magnet. As a result, although I did not get any new result on dHvA of Copper, I had a great experience in doing the experiments. I obtained dHvA signals for the (100) direction, corresponding to the (100) belly orbit. For the (111) direction, I obtained the superposition of two signals [(111) belly and neck].

When I taught the Solid State Physics in Binghamton University (SUNY at Binghamton) in 2012, I wanted to give a talk about the Fermi surface of copper. Although I had an experience of doing experiment of de Haas-van Alphen effect around 1975, I do not have any knowledge on the recent progress of the researches on such a study after 1975, since my research was far from the study of Fermiology. So I decided to read an excellent review book written by David Shoenberg entitled Magnetic oscillations in metals (Cambridge, 1984). I also read many recent textbooks on solid state physics in or der to collect information of the Fermi surface of copper (in particular open orbits in Cu Fermi surface). I was a little bit disappointed with these textbooks since almost all the figures on the fermi surface of Cu were copied from figures from Pippard's papers and Shoenberg's papers.

When I read the book of Shoenberg, I found the remarkably simple analytical representation of the Cu Fermi surface which takes account of the cubic symmetry and multiple connectivity of the surface is a Fourier expansion of the form (Roaf 1962, Halse 1969).

$$
\begin{aligned}
C_0 = {} & 3 - \sum \cos\frac{ak_y}{2}\cos\frac{ak_z}{2} + C_{200}(3 - \sum \cos(ak_x) \\
& + C_{211}(3 - \sum \cos ak_x \cos\frac{ak_y}{2}\cos\frac{ak_z}{2}) \\
& + C_{220}(3 - \sum \cos ak_y \cos ak_z) \\
& + C_{310}(6 - \sum \cos\frac{3ak_y}{2}\cos\frac{ak_z}{2} - \sum \cos\frac{3ak_z}{2}\cos\frac{ak_y}{2}) \\
& + C_{222}(1 - \cos ak_x \cos ak_y \cos ak_z) \\
& + C_{321}(6 - \sum \cos\frac{3ak_x}{2}\cos ak_y \cos\frac{ak_z}{2} - \sum \cos\frac{3ak_z}{2}\cos ak_y \cos\frac{ak_x}{2}) + \ldots
\end{aligned}
$$

Where a is the lattice constant of the conventional cubic unit cell) and C's are adjustable parameters to be fitted to the data. The values of the parameters are chosen by a process of trial and error in which extremal areas for particular orientation of an external magnetic field $\boldsymbol{B}$ are computed for trial values of the parameters and compared with the experimentally measures areas.

Here we use the following values of *C*'s in Fourier representation of the Cu Fermi surface (Coleridge and Templeton 1972);

$$C_0 = 1.691314, \qquad C_{200} = 0.006574, \qquad C_{211} = -0.426081,$$
$$C_{220} = -0.018050 \qquad C_{310} = -0.036283.$$

If one is familiar with the Mathematica program, it occurs to one that the 3D Fermi surface of Cu in the extended zone can be constructed by using the ContourPlot3D program. Once the Fermi surface of Cu is constructed, one can discuss the shape of the extremal orbits which can be observed in the de Haas-van Alphen effect. We use the coefficients which has been reported by Halse and Templeton,and so on. Using this program, we can also find the pattern of the open orbits for the particular directions of the magnetic fields. The cross section of the Fermi surface can be obtained by using the ContourPlot3D and appropriate rotation matrix

$$\begin{pmatrix} k_x \\ k_y \\ k_z \end{pmatrix} = \begin{pmatrix} \cos\theta & -\sin\theta & 0 \\ \sin\theta & \cos\theta & 0 \\ 0 & 0 & 1 \end{pmatrix} \begin{pmatrix} k_x' \\ k_y' \\ k_z' \end{pmatrix}$$

for the rotation of $\boldsymbol{B}$ around the <001> direction with $k_x' = 0$. In this case, we can find the patterns of the open orbits for the directions <100>, <110>, and <010>.

$$\begin{pmatrix} k_x \\ k_y \\ k_z \end{pmatrix} = \begin{pmatrix} \frac{1+\cos\theta}{2} & \frac{-1+\cos\theta}{2} & -\frac{1}{\sqrt{2}}\sin\theta \\ \frac{-1+\cos\theta}{2} & \frac{1+\cos\theta}{2} & -\frac{1}{\sqrt{2}}\sin\theta \\ \frac{1}{\sqrt{2}}\sin\theta & \frac{1}{\sqrt{2}}\sin\theta & \cos\theta \end{pmatrix} \begin{pmatrix} k_x' \\ k_y' \\ k_z' \end{pmatrix}$$

for the rotation of $\boldsymbol{B}$ around the $\langle 1\bar{1}0 \rangle$ direction with $k_z' = 0$. In this case, we can find the patterns of the open orbits for the directions <001>, <111>, and <001>.

((Mathematica))

```
A1 = RotationMatrix[θ, {0, 0, 1}];
A1 // MatrixForm
```

$$\begin{pmatrix} \text{Cos}[\theta] & -\text{Sin}[\theta] & 0 \\ \text{Sin}[\theta] & \text{Cos}[\theta] & 0 \\ 0 & 0 & 1 \end{pmatrix}$$

```
B1 = RotationMatrix[θ, {1, -1, 0}];
B1 // MatrixForm
```

$$\begin{pmatrix} \frac{1}{2}\,(1+\text{Cos}[\theta]) & \frac{1}{2}\,(-1+\text{Cos}[\theta]) & -\frac{\text{Sin}[\theta]}{\sqrt{2}} \\ \frac{1}{2}\,(-1+\text{Cos}[\theta]) & \frac{1}{2}\,(1+\text{Cos}[\theta]) & -\frac{\text{Sin}[\theta]}{\sqrt{2}} \\ \frac{\text{Sin}[\theta]}{\sqrt{2}} & \frac{\text{Sin}[\theta]}{\sqrt{2}} & \text{Cos}[\theta] \end{pmatrix}$$

Using the Mathematica, we will discuss the following.

(i) dHvA orbits for the particular orientation of the magnetic fields;
  (a) Belly, neck, and 6-cornered rosette for the <111> directions
  (b) Belly and 4-cornered rosette for the <100> direction
  (c) Dog's bone and lemon

(ii) Evidence of the lemon orbits for the <110> direction
  Making a plot of cross section of Cu Fermi surface as a function of the magnitude of k_B.

(iii) Periodic and aperiodic patterns of open orbits and closed orbits for the (100) plane

(iv) Periodic and aperiodic patterns of open orbits and closed orbits for the $(1\,\bar{1}\,0)$ plane

(v) FFT (Fast Fourier Transform) of the aperiodic patterns.

A part of the purpose of this note is to reproduce the shape of the Fermi surface of Cu which has been determined from the de Haas-van Alphen effect mainly by Shoenberg group. In 1984, Shoenberg published an excellent book entitled

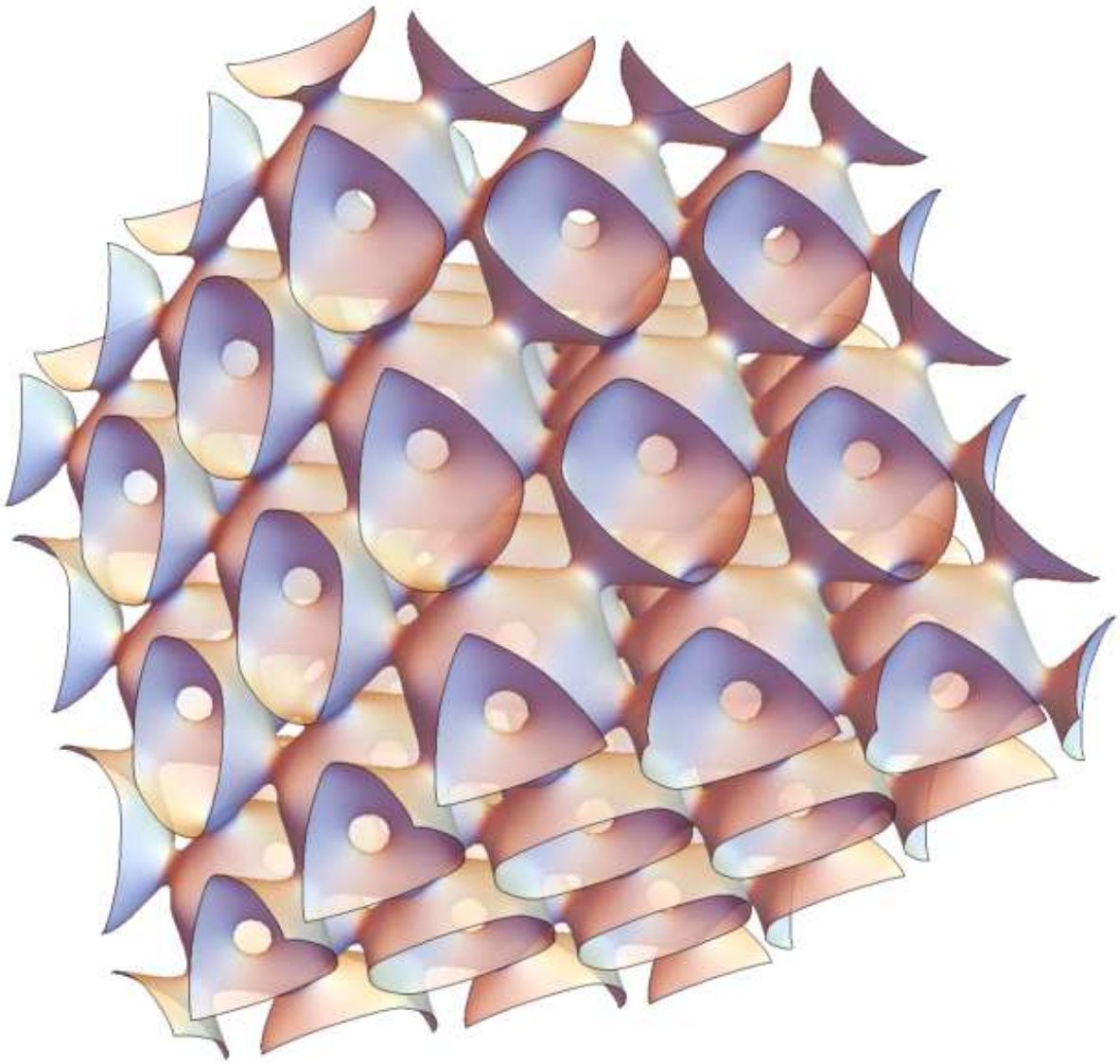

Fig.1 ContourPlot3D for the Cu Fermi surface in the extended zone.

2. Determination of the shape of Fermi surface in Cu (Pippard,Shoenberg and so on)

The de Haas van Alphen effect of Copper was first observed by David Shoenberg. The Fermi surface of the copper was determined experimentally.

D. Shoenberg:Phil. Trans. Roy. Soc. A 255, 85-133 (1962)

"Following the discovery of the effect in copper, silver and gold by the impulsive high-field method, a study of the variation of the oscillatory frequency (which is proportional to the extremal area of cross-section of the Fermi surface by planes normal to the field) with the direction of the magnetic field relative to the crystal axes has made possible a detailed determination of the Fermi surfaces of these metals. As well as high-frequency oscillations associated with major ('belly')

sections of the Fermi surface, low frequency oscillations are observed for the field in the [111] direction, which can be associated with the 'necks' in which the Fermi surface makes contact with the hexagonal faces of the Brillouin zone, as suggested by Pippard. The general topology of Pippard's model is confirmed by the existence of medium frequencies for the field along [100] and [110], which can be associated with 'hole' sections having the shape of a 'rosette' and a 'dog's bone', respectively. By making the high-frequency belly oscillations beat with the oscillations from a reference specimen, it has proved possible to measure the small variations of the belly frequency with field direction, which amount to only a few parts per cent, with an accuracy of a few parts per cent."

3. Free electron Fermi sphere for Cu with fcc lattice

$$2\frac{V}{(2\pi)^3}\frac{4\pi}{3}k_F{}^3 = 4p\frac{V}{a^3}$$

or

$$k_F = \frac{2\pi}{a}\left(\frac{3p}{2\pi}\right)^{1/3}, \qquad \varepsilon_F = \frac{\hbar^2}{2m}\left(\frac{2\pi}{a}\right)^2\left(\frac{3p}{2\pi}\right)^{2/3} = E_0\left(\frac{3p}{2\pi}\right)^{2/3}$$

where p is the number of electrons per atom and E_0 is defined by

$$E_0 = \frac{\hbar^2}{2m}\left(\frac{2\pi}{a}\right)^2$$

When $p = 1$ for Cu, then we have

$$k_F = \frac{2\pi}{a}\left(\frac{3}{2\pi}\right)^{1/3} = \frac{4.91089}{a} = 1.36036 \text{ x } 10^8 \text{ cm}^{-1}$$

where the lattice constant of Cu (for the conventional unit cell for fcc) is given by

$a = 3.61$ Å.

The area is evaluated as

$$A = \pi k_F{}^2 = 5.81375 \text{ x } 10^{16} \text{ cm}^{-2}$$

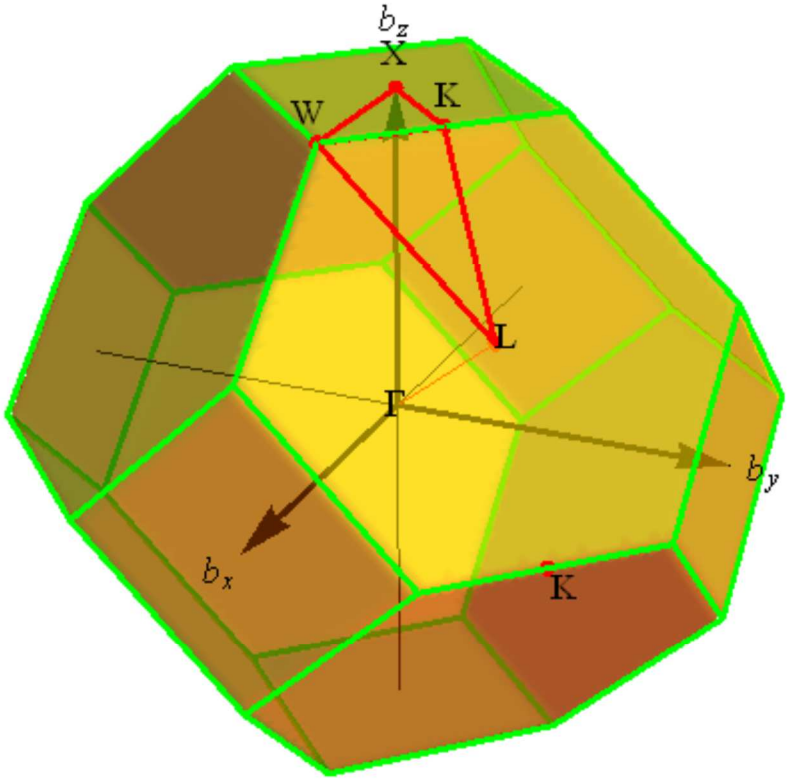

Fig.2 Brillouin zone of the fcc lattice (Cu, typically). ***X*** = (0,0,1), ***W*** = (1/2, 0, 1), ***L*** = (1/2, 1/2, 1/2), ***K*** = (1/4, 1/4, 1) or ***K*** = (3/4, 3/4, 0). $\Gamma L = \sqrt{3}/2 = 0.866$, in the units of $2\pi/a$, where a is the conventional lattice cell.

The shortest distance across the Brillouin zone is

$$\Gamma\mathrm{L} = \frac{\sqrt{3}}{2}\frac{2\pi}{a} = \frac{5.4414}{a}$$

which is larger than the radius k_F for the free electron Fermi sphere; $k_F = \frac{4.91089}{a}$. The Fermi sphere does not touch the zone boundary, but we know that the presence of a zone boundary tends to lower the band energy near the boundary. Thus it is reasonable that the Fermi surface neck out to meet the closest face (the hexagonal with the L point) of the zone.

The square faces (with X point) is

$$\Gamma X = \frac{2\pi}{a} = \frac{6.2836}{a}$$

So the Fermi surface does not neck out to meet these square faces.

4. dHvA frequency (experiment) for Cu

The dHvA frequency and the corresponding area are determined from the de Haas-van Alphen effect. The dHvA frequency F(in the units of G) is related to the extremal cross-sectional area A (in the units of cm^{-2}) in the $\boldsymbol{k}$-space normal to the direction of the magnetic field. B,

$$F = \frac{\hbar c}{2\pi e} A \,.$$

where [$\hbar$]=erg sec, [c] = cm/s. [e] = G cm^2.

Here is the result for Cu (Joseph et al., 1966),

$F(D_{110}) = 2.5203 \times 10^7$ G $A(D_{110}) = 2.40584 \times 10^{15}$ cm^{-2}
$F(B_{111}) = 5.8468 \times 10^8$ G $A(B_{111}) = 5.58127 \times 10^{16}$ cm^{-2}
$F(N_{111}) = 2.1872 \times 10^7$ G $A(N_{111}) = 2.08787 \times 10^{15}$ cm^{-2}
$F(B_{100}) = 6.0337 \times 10^8$ G $A(B_{100}) = 5.75969 \times 10^{16}$ cm^{-2}

where D_{110} denotes the dog's bone orbit for $\boldsymbol{B}$//<110> direction, B_{100} denotes the belly orbit for B//<100> direction, and B_{111} denotes the belly orbit for B//<111> direction, and N_{111} denotes the neck orbit. We note that

$$\frac{A(B_{111})}{A(N_{111})} = \frac{5.58127 \times 10^{16}}{2.08787 \times 10^{15}} = 26.7$$

We calculate the typical values for the period of B at B = 5 T: From the formula

$$\Delta \frac{1}{B} = \frac{1}{F} = \frac{2\pi e}{\hbar c A}$$

we get

$$\Delta B \approx \frac{2\pi e}{\hbar c A} B^2$$

$\Delta B(D_{110}) =$ 99.19 G
$\Delta B(B_{111}) =$ 4.276 G
$\Delta B(N_{111}) =$ 114.3 G
$\Delta(B_{100}) =$ 4.14 G

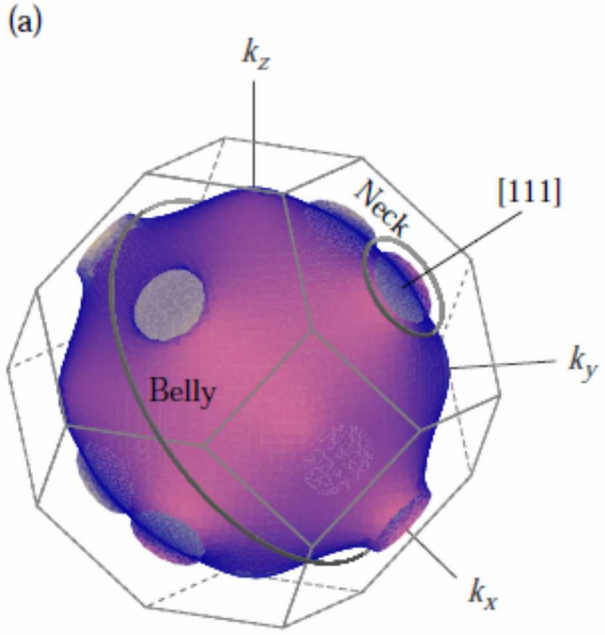
(a)
k_z
Neck
[111]
k_y
Belly
k_x

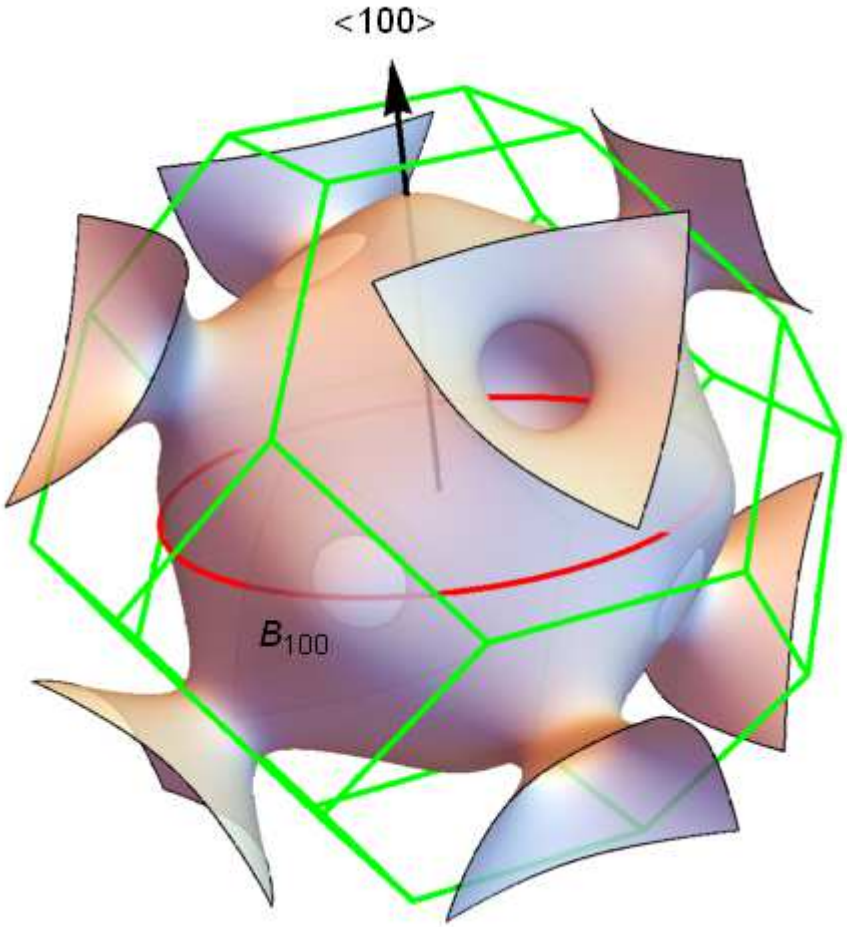

Fig.3 Belly (B) orbit for the <100> direction.

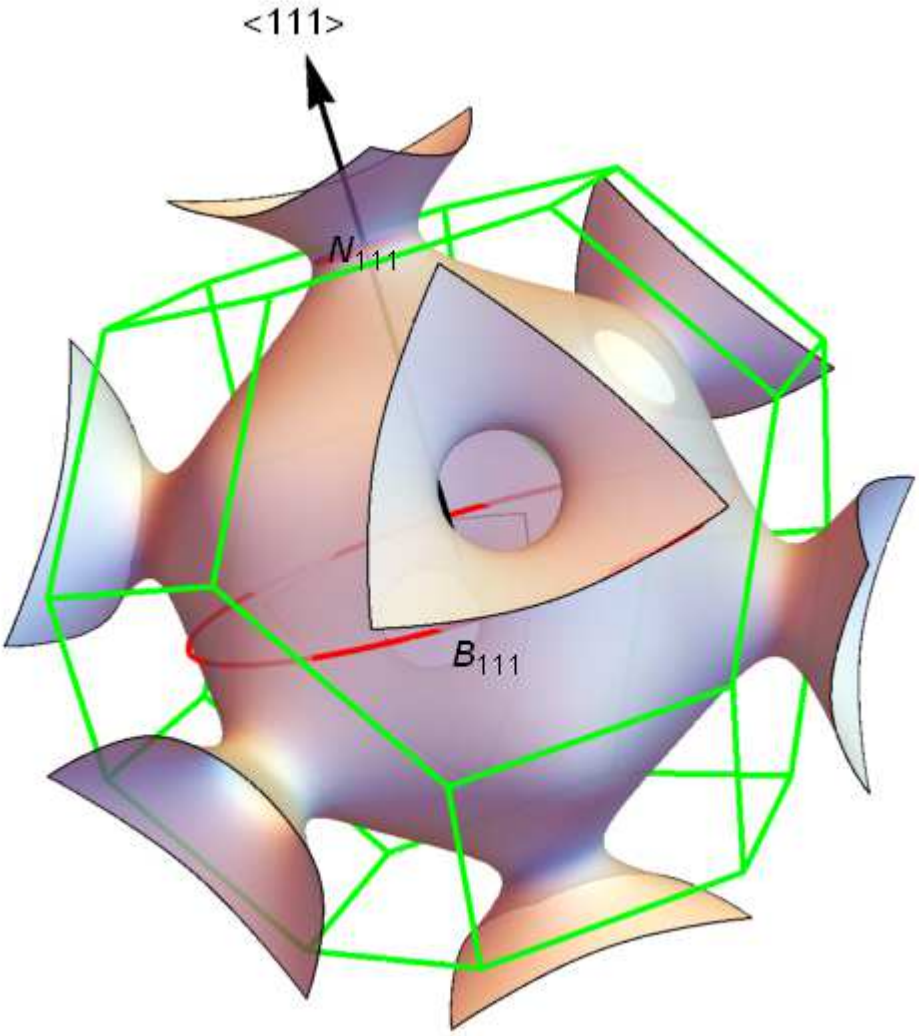

Fig.4 Belly (B) orbit and neck (N) orbit for the <111> direction.

5. dHvA orbits for the <100> direction

About the main symmetry directions <100> there exist four-cornered rosette hole orbit, with the corners provided by the bulges.

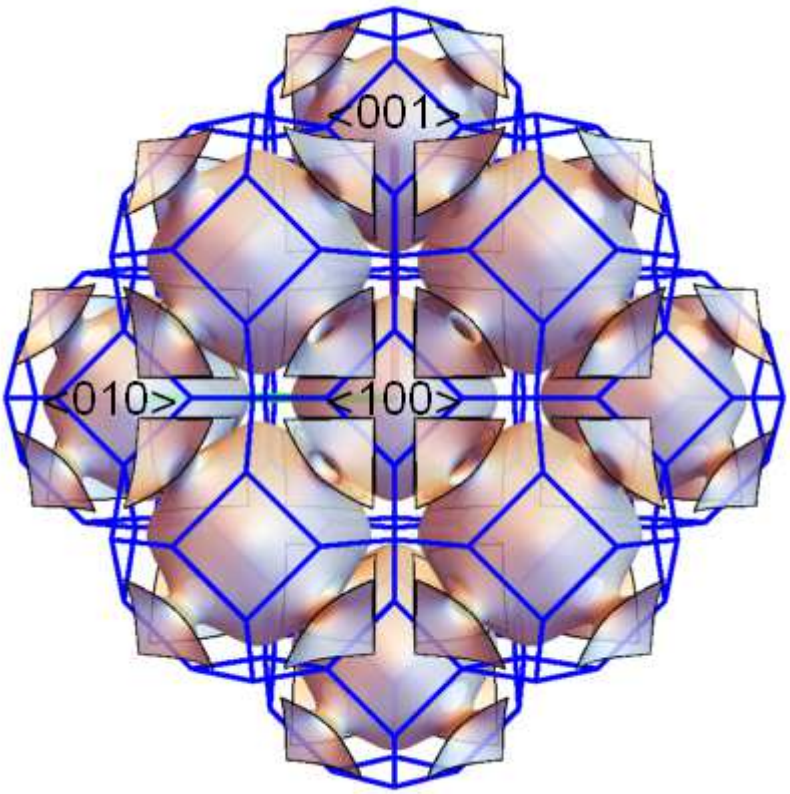

Fig.5 Four-cornered rosette (4-R) for the <100> direction for Cu Fermi surface in the extended scheme (in the present work)

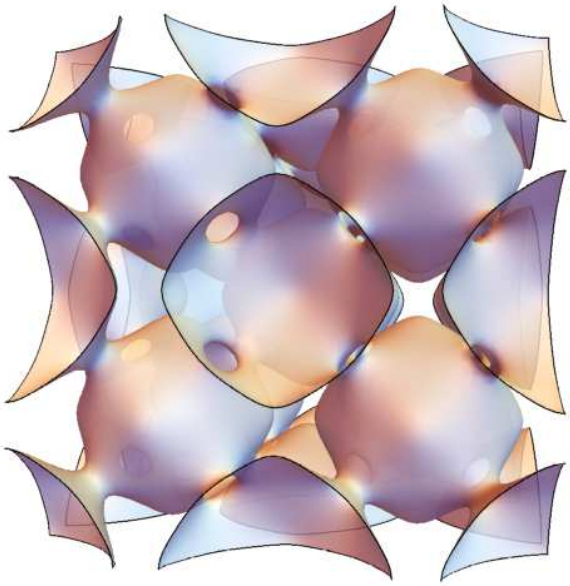

Fig.6 Four-cornered rosette (4-R) for the <100> direction for Cu Fermi surface in the extended scheme (in the present work)

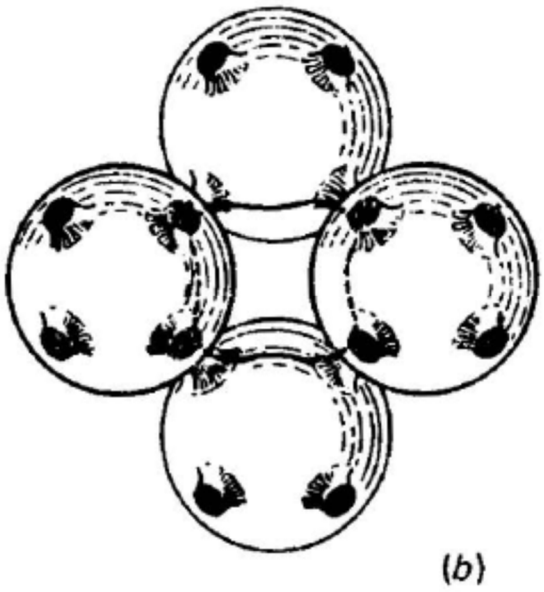

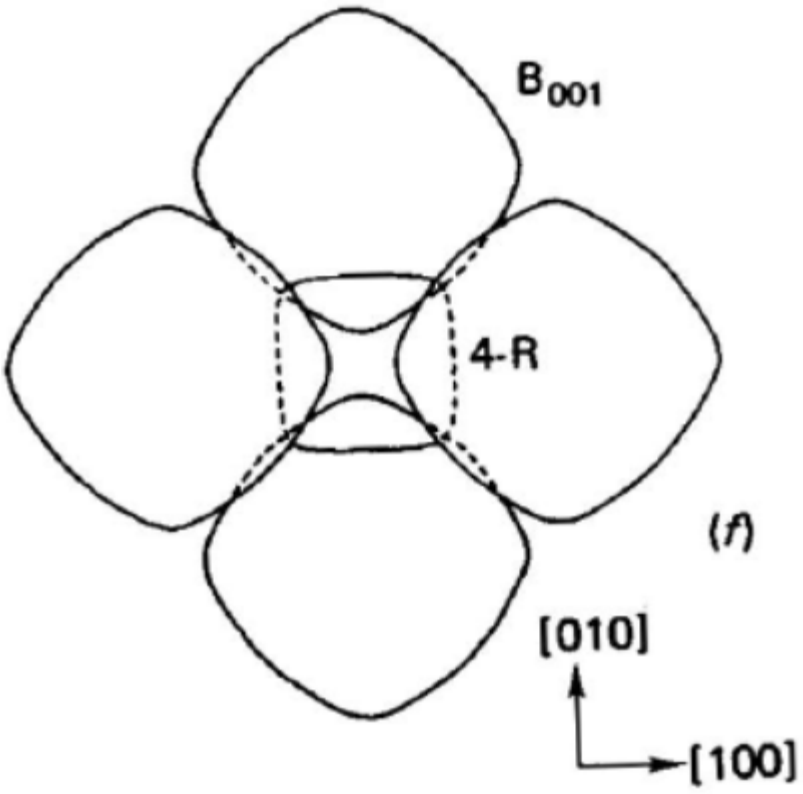

Fig.7 Four-cornered rosette (6-R) orbit for the <100> direction for Cu Fermi surface in the extended scheme (Shoenberg,1984)

First we make a plot of the Fermi surface in the first Brillouin zone centered at the origin O. The Fermi surface in the extended scheme can be constructed by translating the Fermi surface at the origin into the nine reciprocal lattices defined by

$$\boldsymbol{b}_1,\ -\boldsymbol{b}_3,\ -\boldsymbol{b}_4,\ -\boldsymbol{b}_2,\ -(\boldsymbol{b}_1+\boldsymbol{b}_2),\ \boldsymbol{b}_1+\boldsymbol{b}_2,\ -(\boldsymbol{b}_3+\boldsymbol{b}_1),\ \boldsymbol{b}_3+\boldsymbol{b}_1,$$

where

$$\boldsymbol{b}_1=\frac{2\pi}{a}(-1,1,1)\,,\qquad \boldsymbol{b}_2=\frac{2\pi}{a}(1,-1,1)\,,\qquad \boldsymbol{b}_3=\frac{2\pi}{a}(1,1,-1)$$

and

$$\boldsymbol{b}_4=\boldsymbol{b}_1+\boldsymbol{b}_2+\boldsymbol{b}_3=\frac{2\pi}{a}(1,1,1)$$

$$\boldsymbol{b}_1+\boldsymbol{b}_2=\frac{2\pi}{a}(0,0,2),\qquad \boldsymbol{b}_2+\boldsymbol{b}_3=\frac{2\pi}{a}(2,0,0),\qquad \boldsymbol{b}_3+\boldsymbol{b}_1=\frac{2\pi}{a}(0,2,0)$$

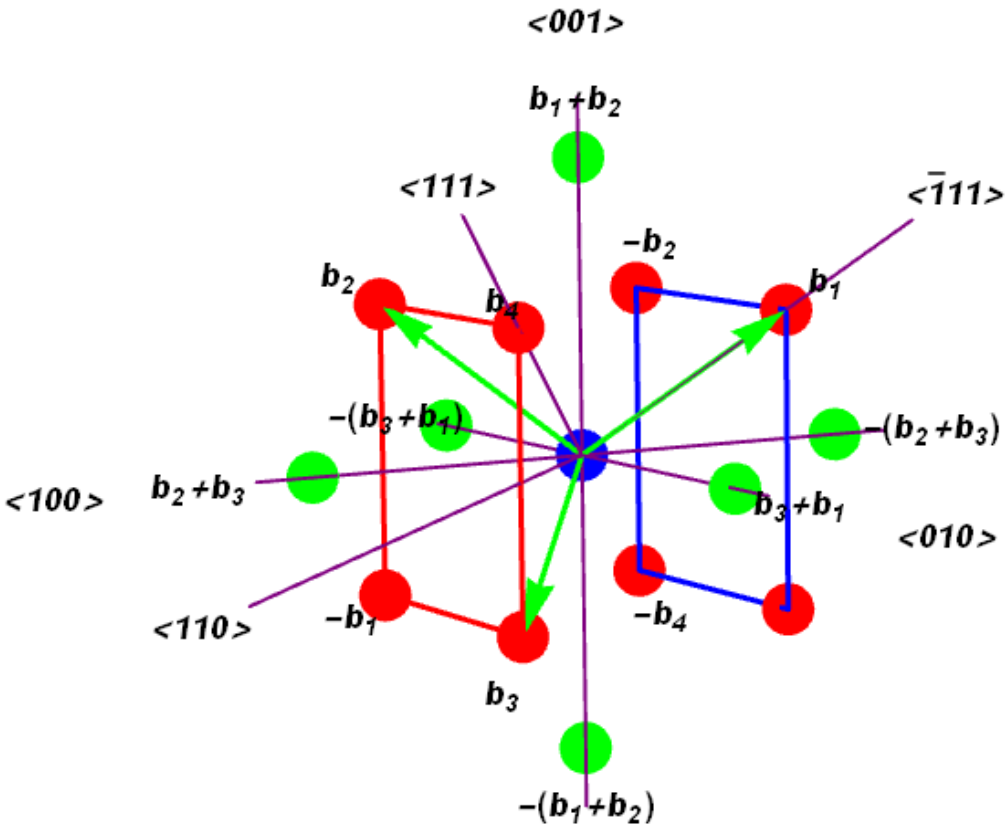

Fig.8 Reciprocal lattice vectors for the fcc lattice(typically Cu) in the unit of $2\pi/a$.

4 dHvA orbits for *B*//<111>

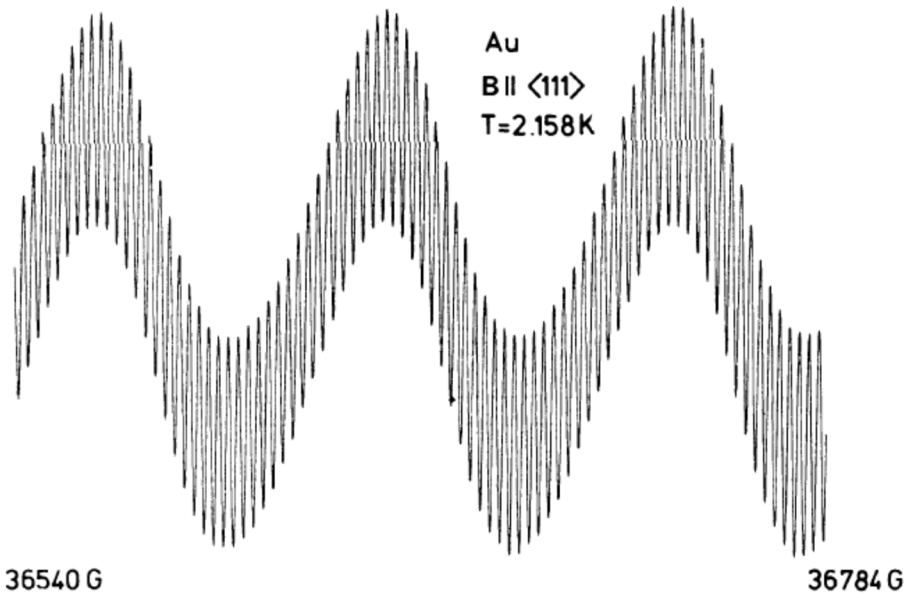

Fig.9 dHvA spectrum for the magnetic field along the <111> direction, for Au. The dHvA signal in Cu is similar to that in Cu. Superposition of the signal from the neck (low frequency) and the belly (high frequency).

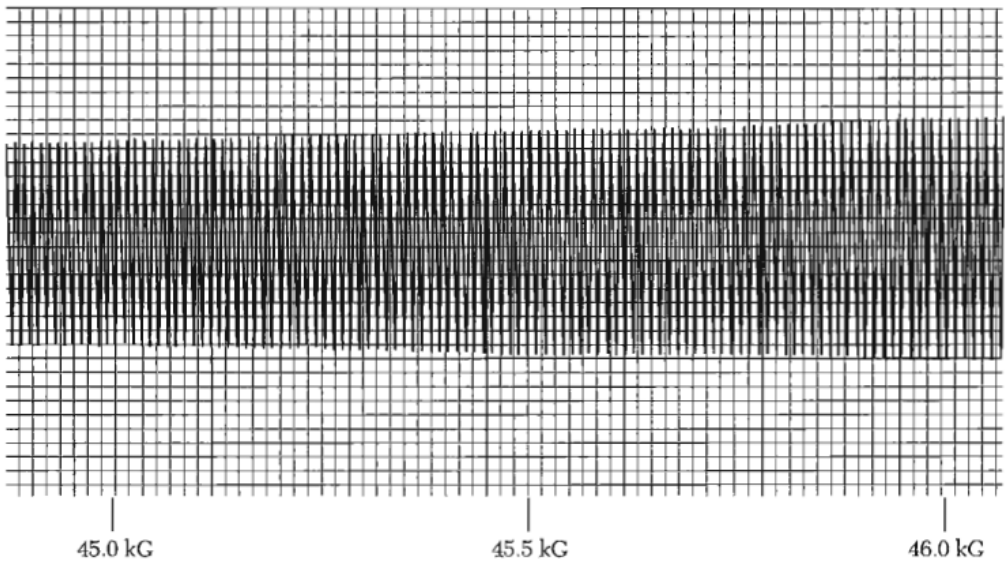

Fig.10 dHvA effect in Au with *B*//<110>. The oscillation is from the dog's bone (hole orbit).[C. Kittel, ISSP, by I.M. Templeton]. The dHvA signal in Cu is similar to that in Au.

The six cornered rosette orbit are about the <111> directions. The view of the Fermi syrface in the <111> direction is shown above. with the six-cornered rosette orbit. Note that the six cornerers are

produced by the bulges of the Fermi surface. This is a hole orbit because the states enclosed by it is not occupied by electrons in the ground state.

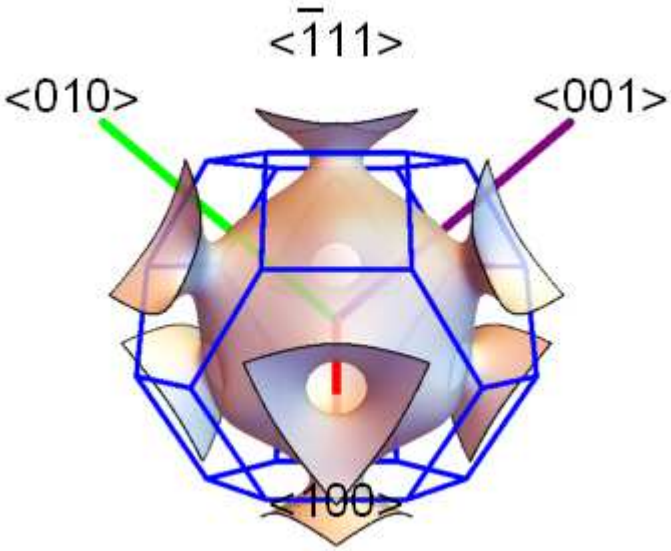

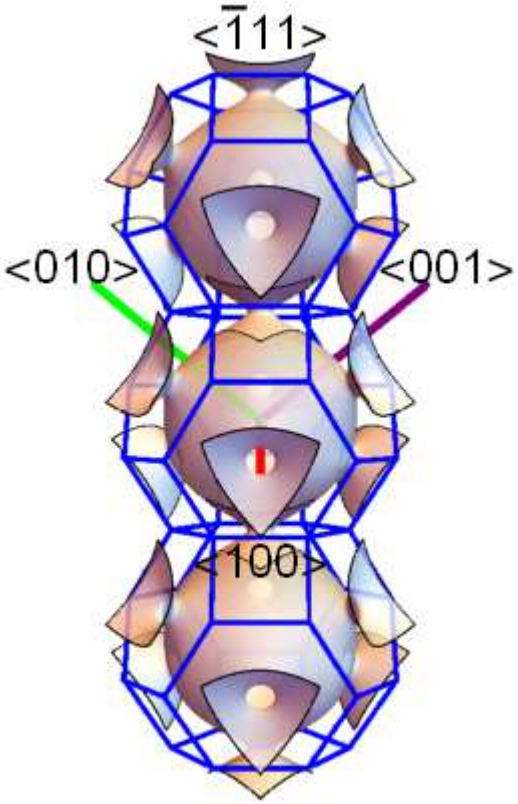

Fig.11 The region of neck at the *L* point. The neighboring Brillouin zones (in the extended scheme) are connected through the neck.

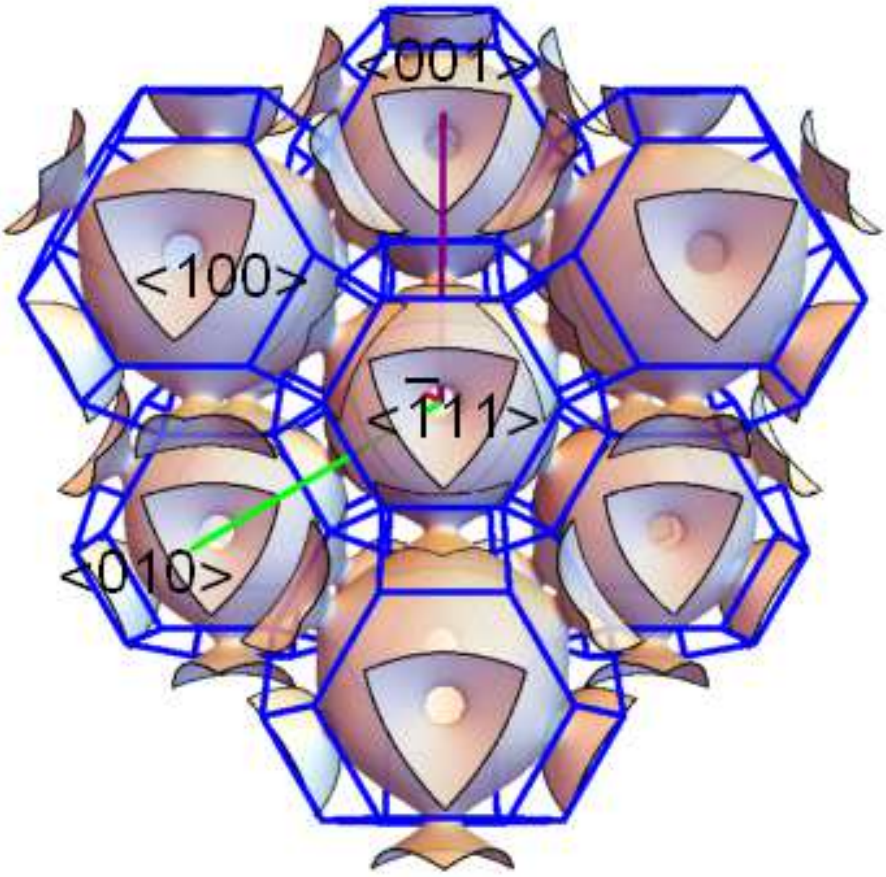

Fig.12 Six-cornered rosette (6-R) orbit for the <111> direction for Cu Fermi surface in the extended scheme. (the present work)

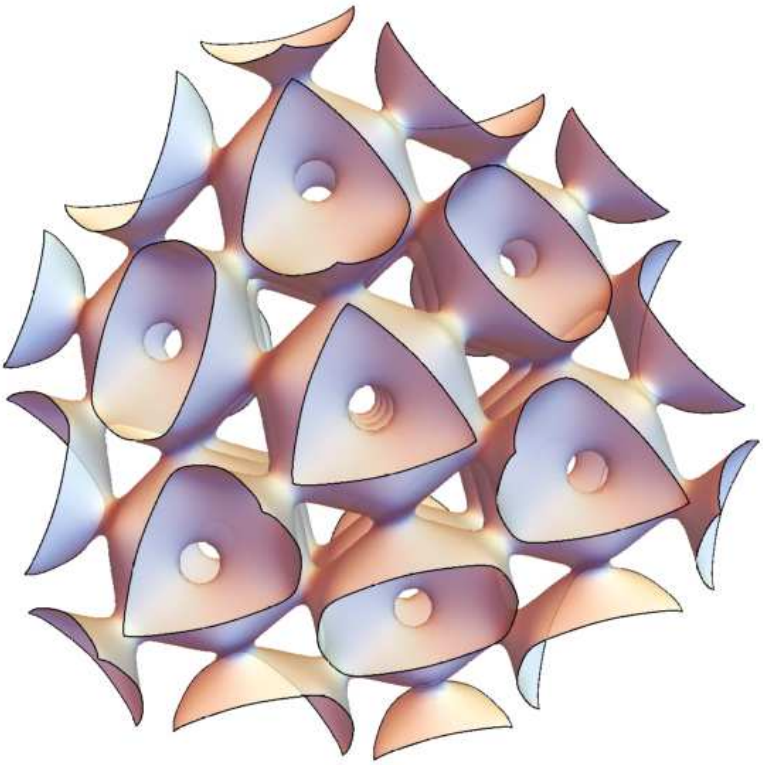

Fig.13 Six-rosette (6-R) orbit for the <111> direction (in the present work)

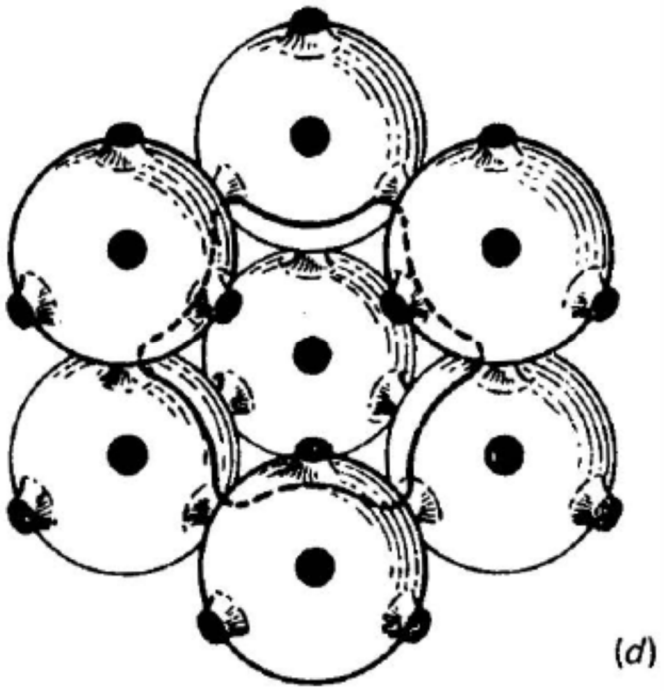

Fig.14 Six-rosette (6-R) orbit for the <111> direction. (Shoenberg, 1984).

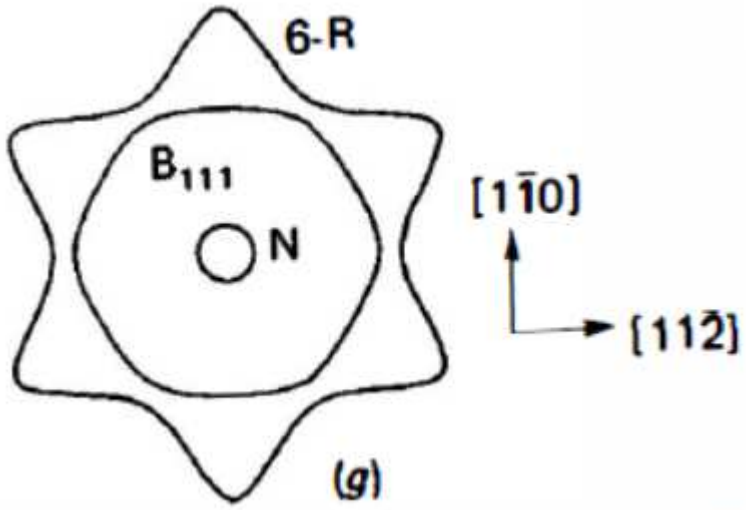

Fig.15 Six-rosette (6-R) orbit, neck (N) orbit, and belly (B) orbit for the <111> direction. (Shoenberg, 1984).

5. The geometry for B//<110>

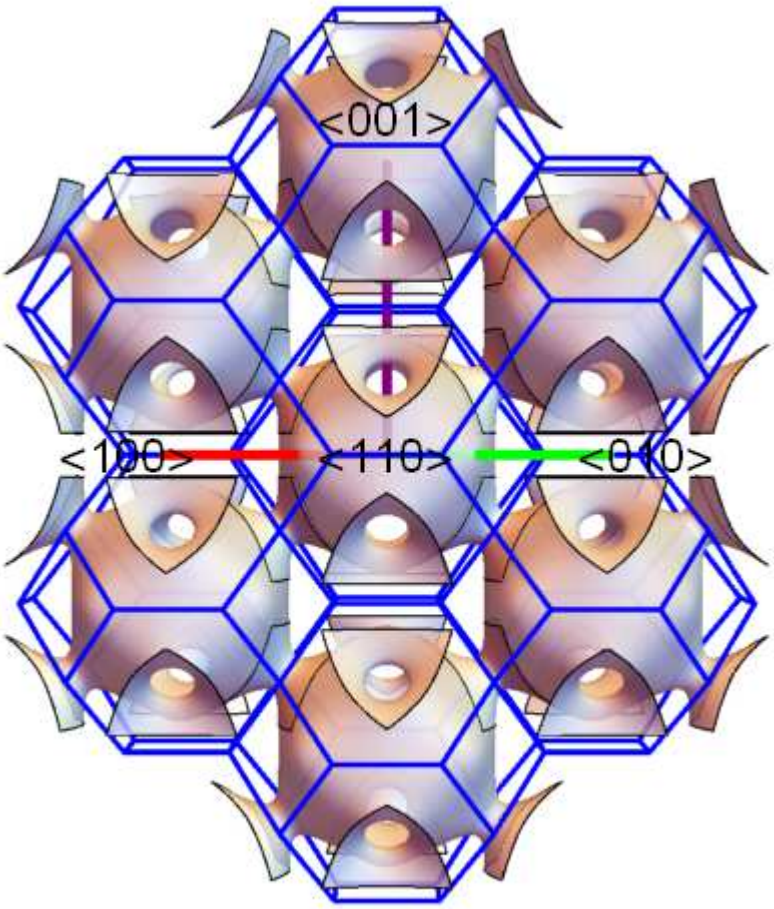

Fig.15 Dog's (D) bone (hole orbit) for the <110> direction (in the present work).

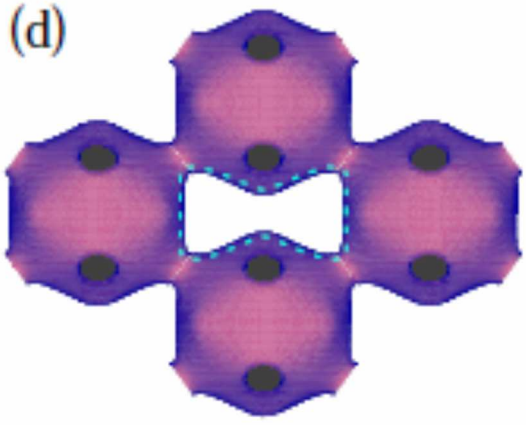

Fig.16 Dog's bone (hole orbit) for the <110> direction (Han, 2013).

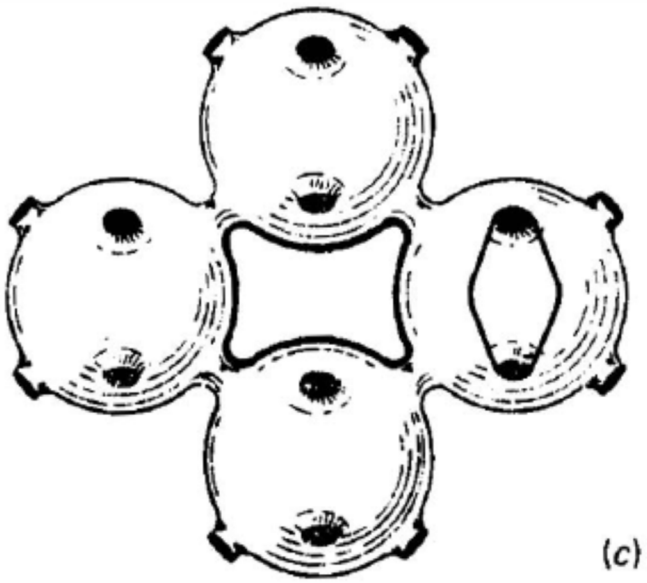

Fig.17 Dog’s bone (hole orbit) for the <110> direction (Shoenberg,1984). Dog’s bone (hole) orbit for the magnetic direction along the <110> direction. The region of the dog's bone is enclosed by the nearest neighbor Brillouin zones in the extended done scheme.

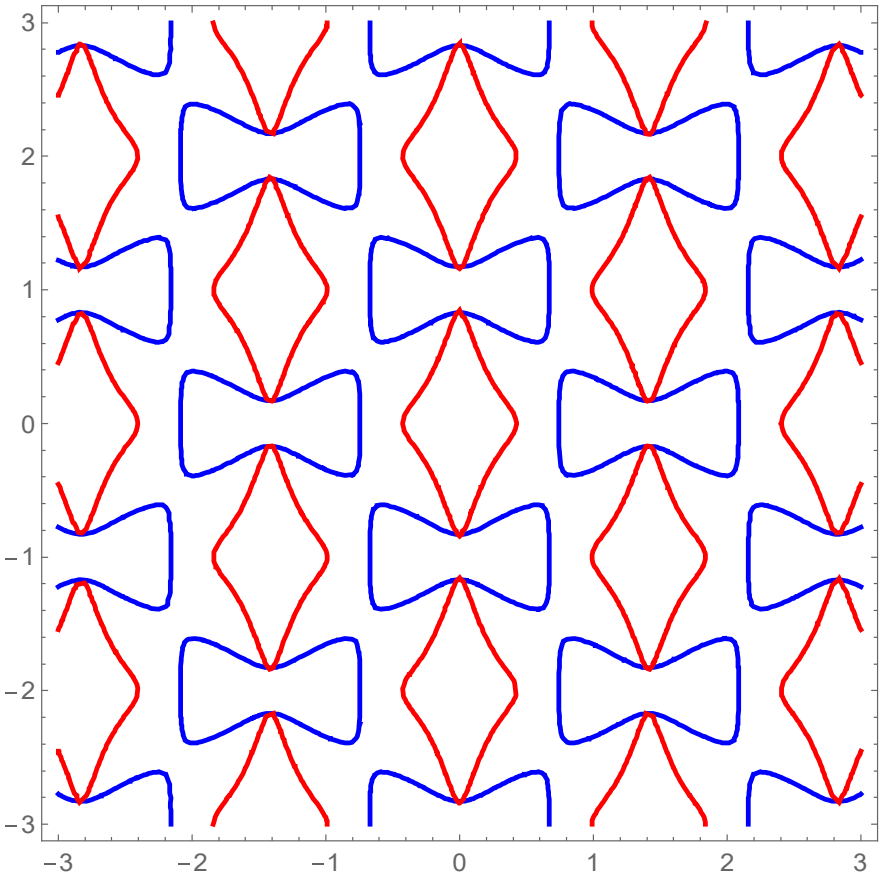

Fig.18 Cross section of the Fermi surface of Cu for the direction of the magnetic field along the <110> direction. $k_B = 0$ for the dog's bone orbit and $k_B = 0.67$ for the lemon (L) orbit (k_B in the units of $2\pi/a$) in the present work. The detail for this plot will be discussed later.

The lemon (e) orbits in the extended zone scheme

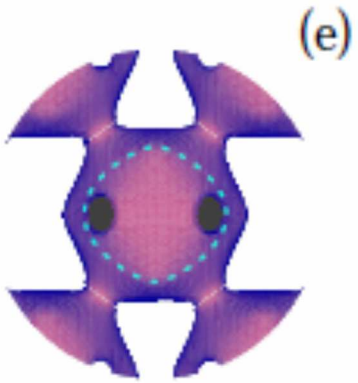

Fig.19 The lemon (L) orbit for the <110> direction (Han, 2013).

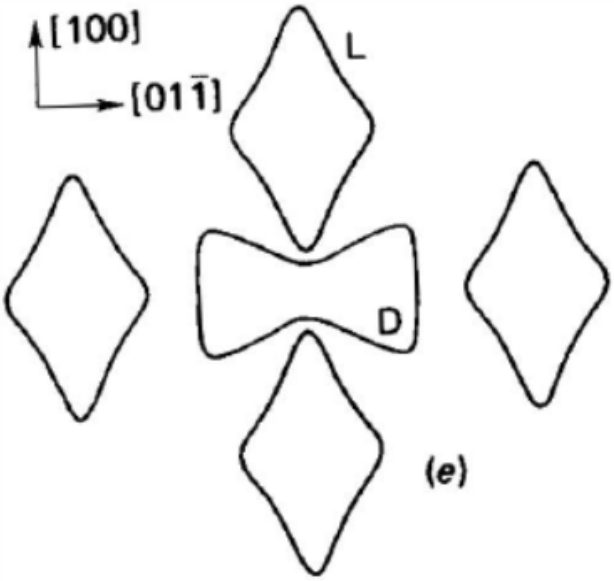

Fig.20 The lemon (L) orbit for the <110> direction. (Shoenberg, 1984). Note that the dog's bone orbit and the lemon orbit are not in the same plane.

6. dHvA results from Joseph and Thorsen

(a) (110) plane

Joseph and Thorsen have measured the dHvA frequenc F (in the units of 10^8 G) for Cu when the magnetic field is applied in the (110) plane, which includes the directions; <001>, <211>, <111>, and <110>. Their results are as follows.

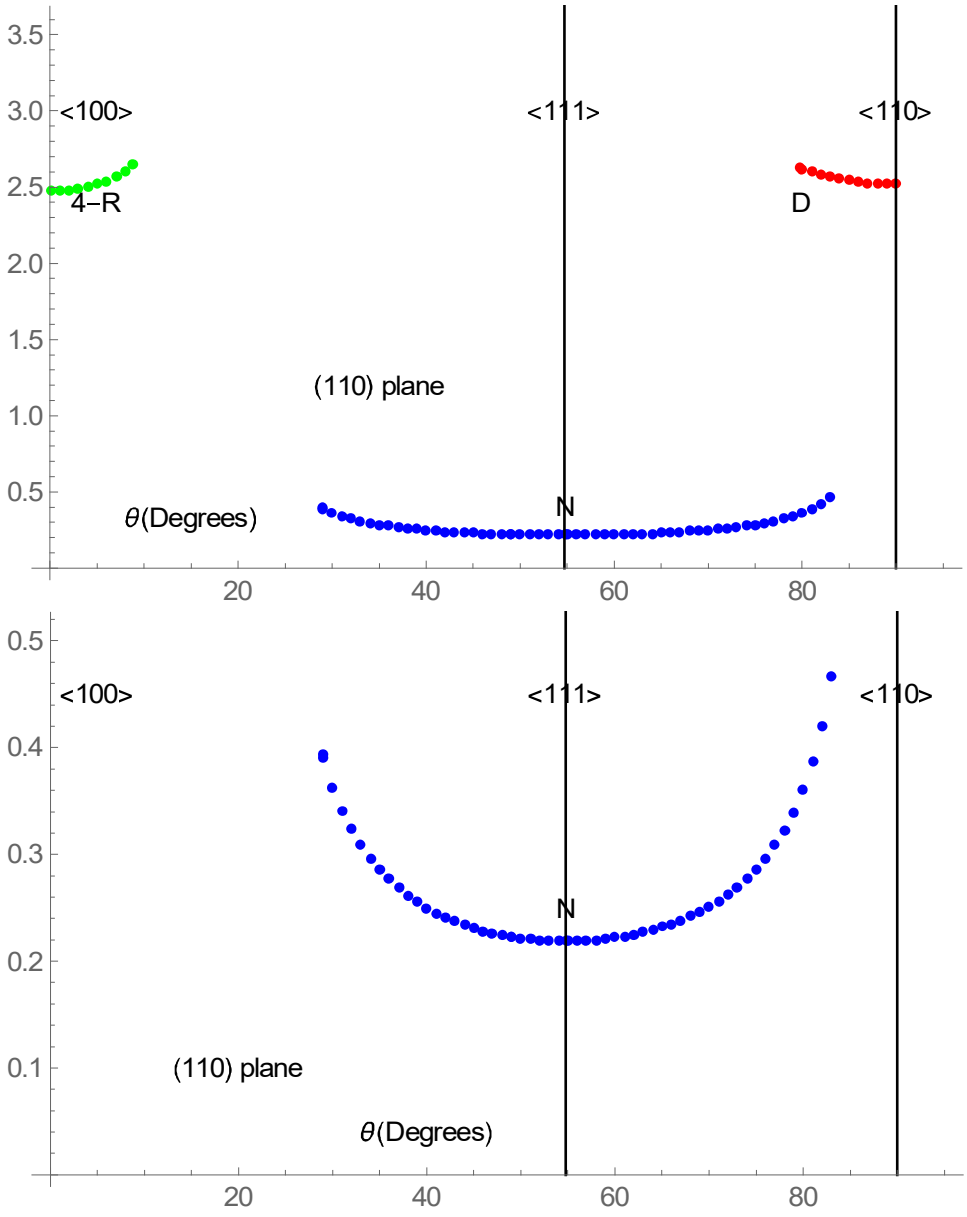
3.5
3.0
2.5
2.0
1.5
1.0
0.5
<100>
<111>
<110>
4−R
D
(110) plane
θ(Degrees)
N
20
40
60
80
0.5
0.4
0.3
0.2
0.1
<100>
<111>
<110>
N
(110) plane
θ(Degrees)
20
40
60
80

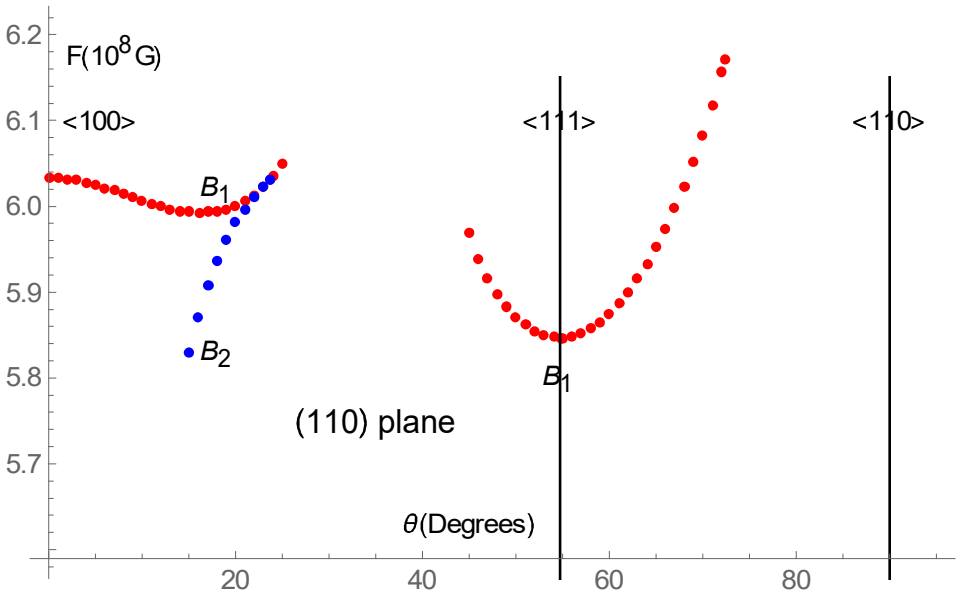

Fig.21 dHvA frequency [$F(10^8$ G)] as a function of angle where the magnetic field is rotated in the (110) plane. Joseph and Thorsen (1966). B_1 and B_2 (belly).4-R (four-cornered rosette). N (neck). D (dog's bone).

(b) (100) plane

Joseph and Thorsen also have measured the dHvA frequenc F (in the units of 10^8 G) for Cu when the magnetic field is applied in the (100) plane, which includes the directions; <100>, <110>, and <010>. Their results are as follows.

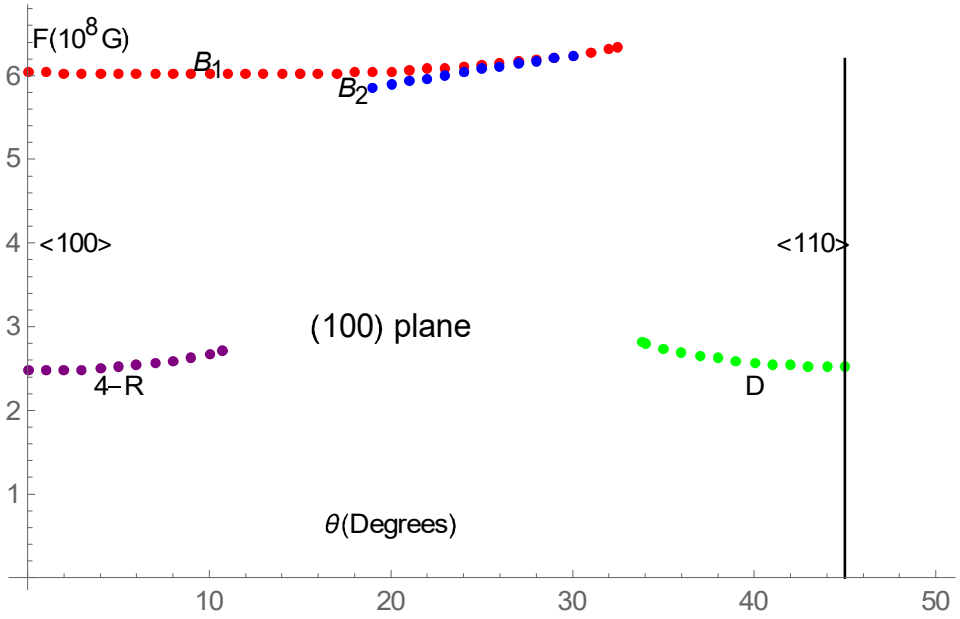

Fig.22 dHvA frequency as a function of angle where the magnetic field is rotated in the (100) plane. Joseph and Thorsen (1966). B_1 and B_2 (belly).4-R (four-cornered rosette). D (dog's bone).

7. Lemon orbit for the <110> direction

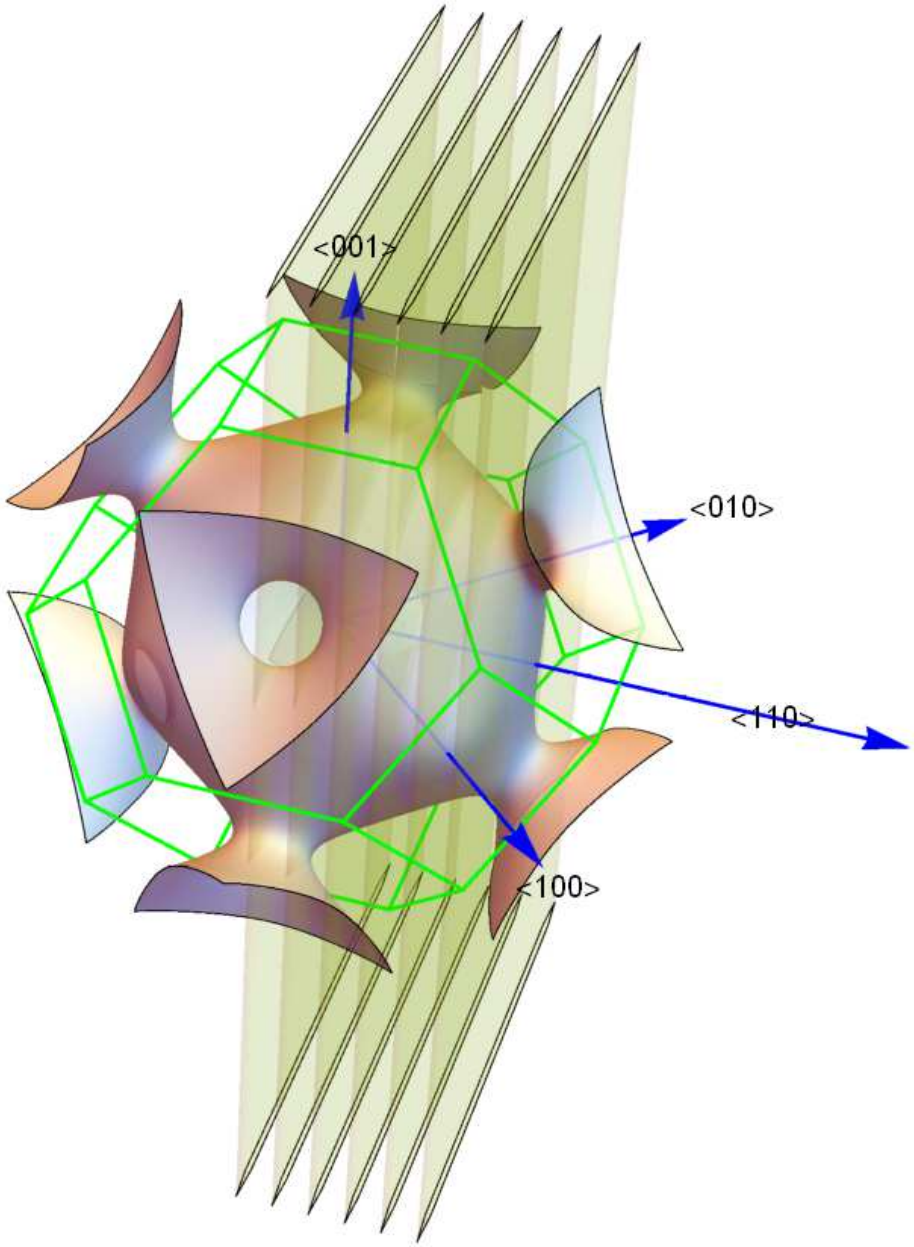

$k_B = 0.0$

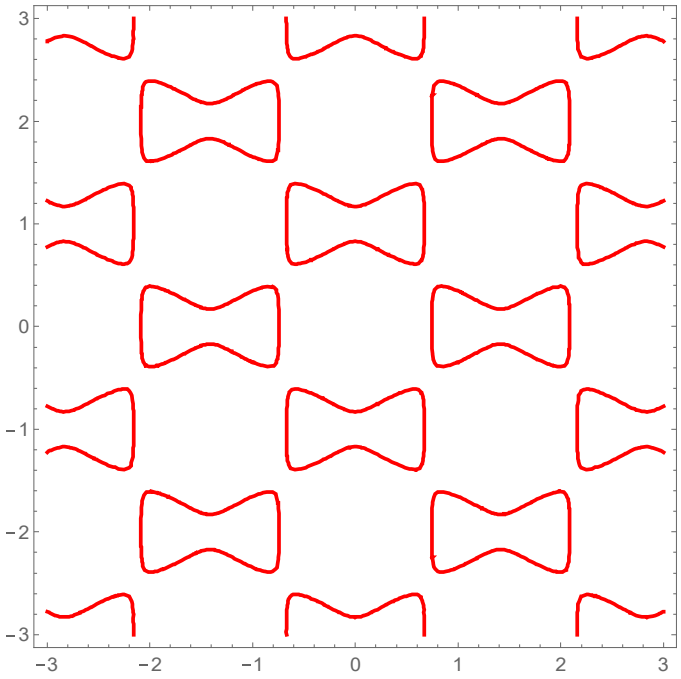

$k_B = 0.14$

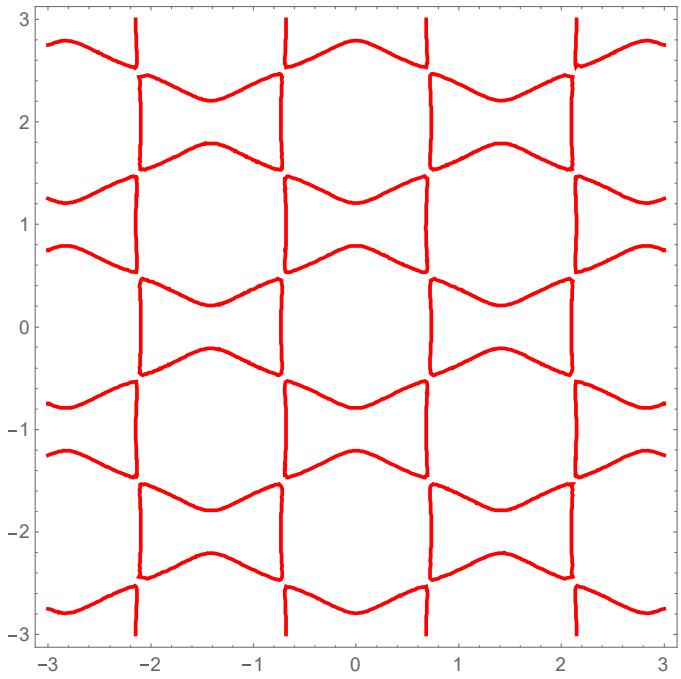

$k_B = 0.16$

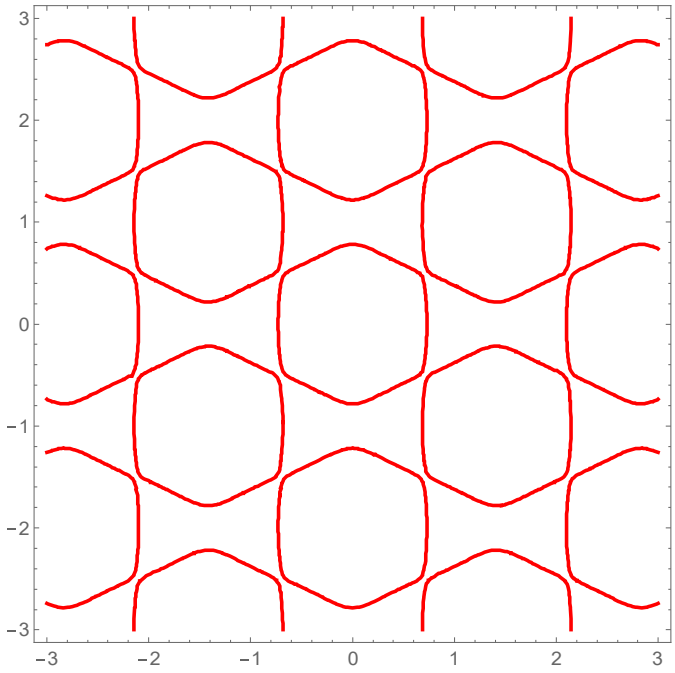

$k_B = 0.20$

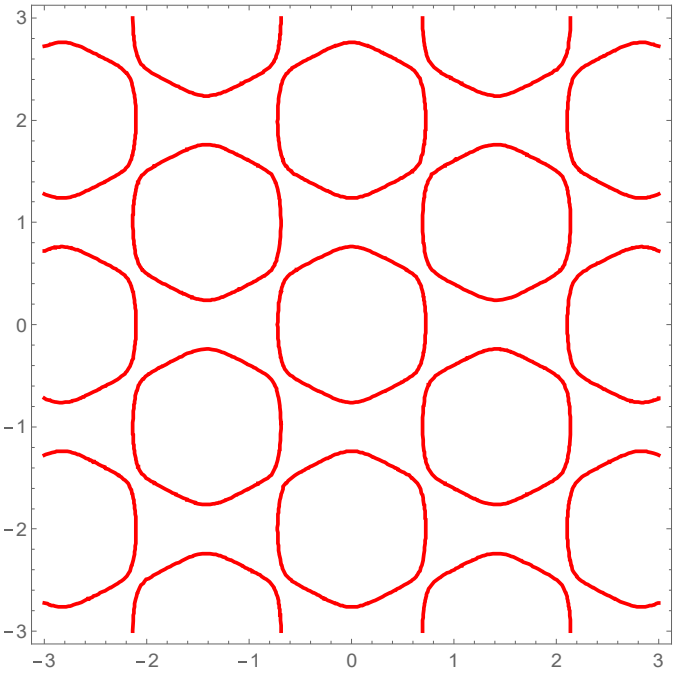

$k_B = 0.32$

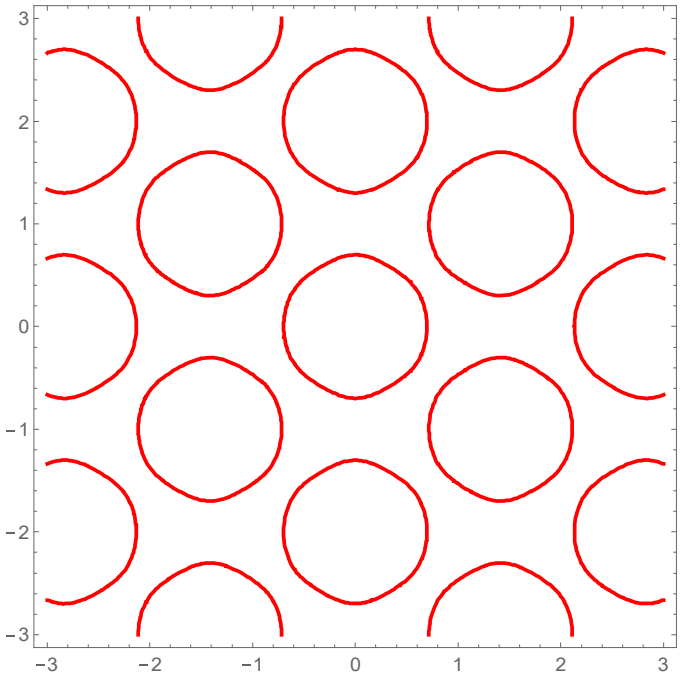

$k_B = 0.54$

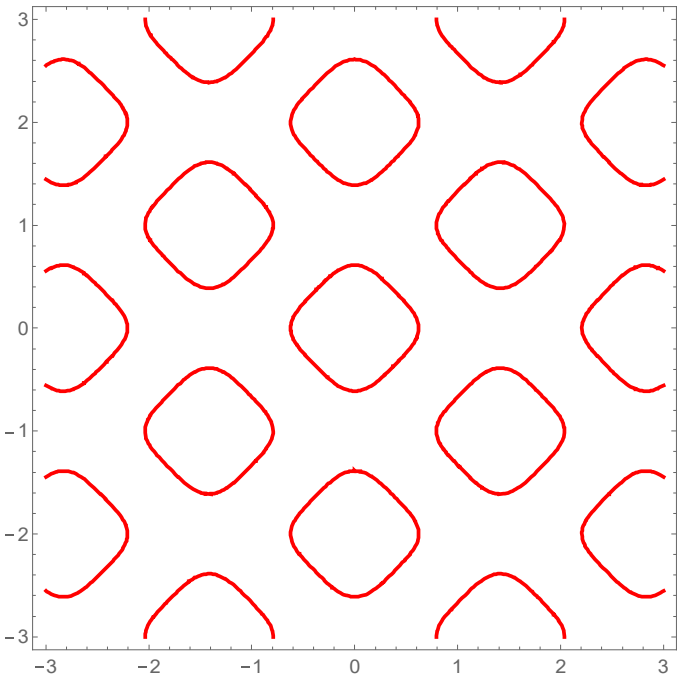

$k_B = 0.58$

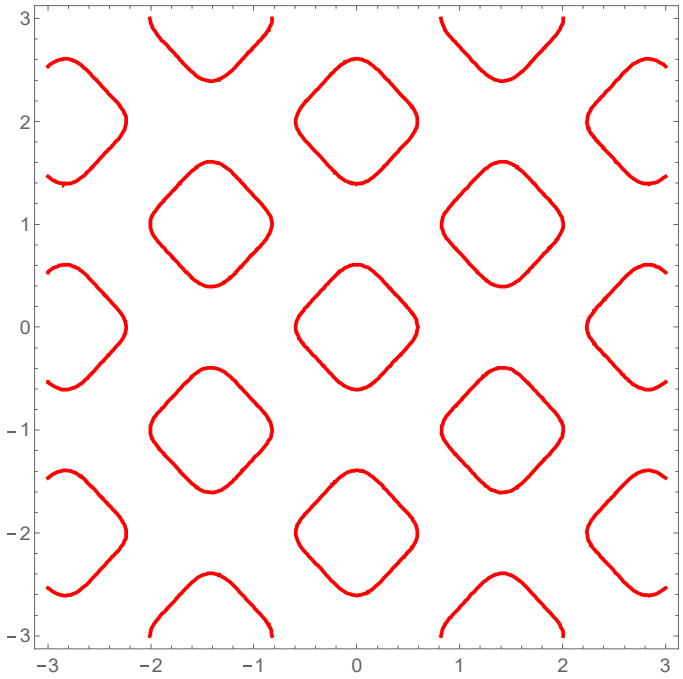

$k_B = 0.62$

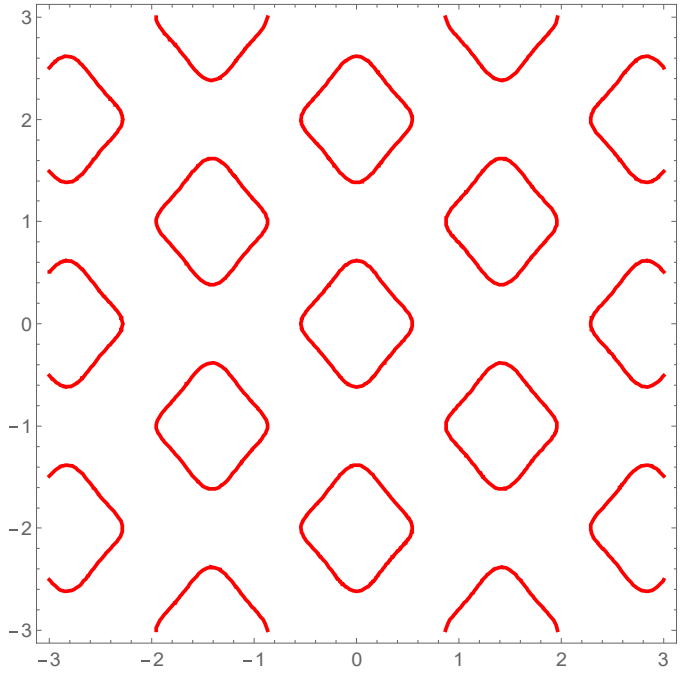

$k_B = 0.65$

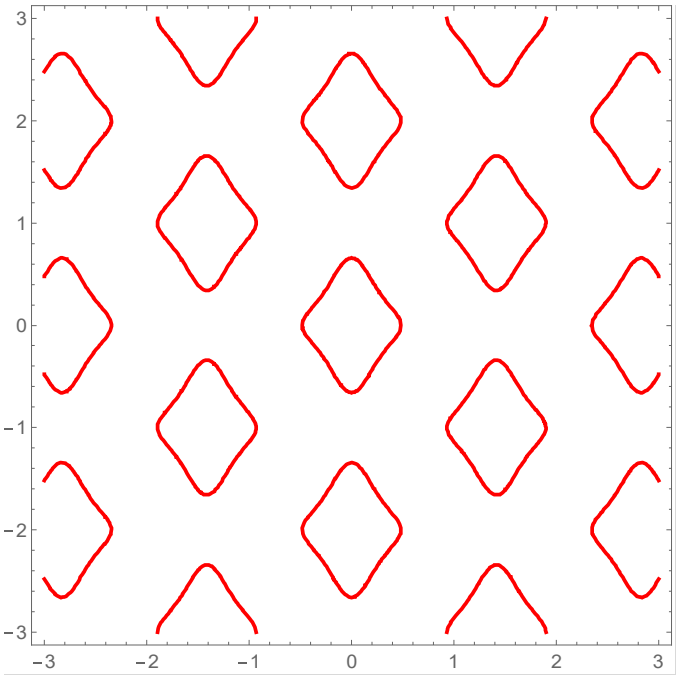

$k_B = 0.67$

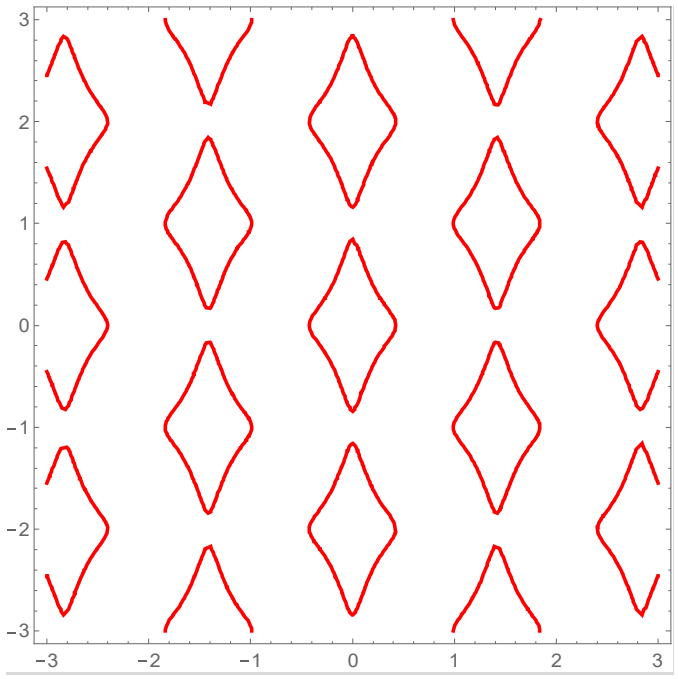

$k_B = 0.672$

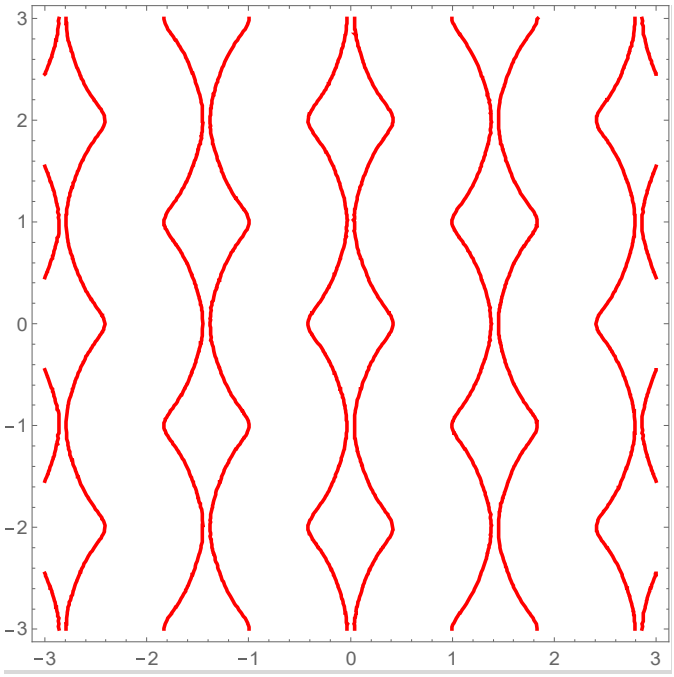

Superposition of
$k_B = 0.67$ and $k_B = 0$

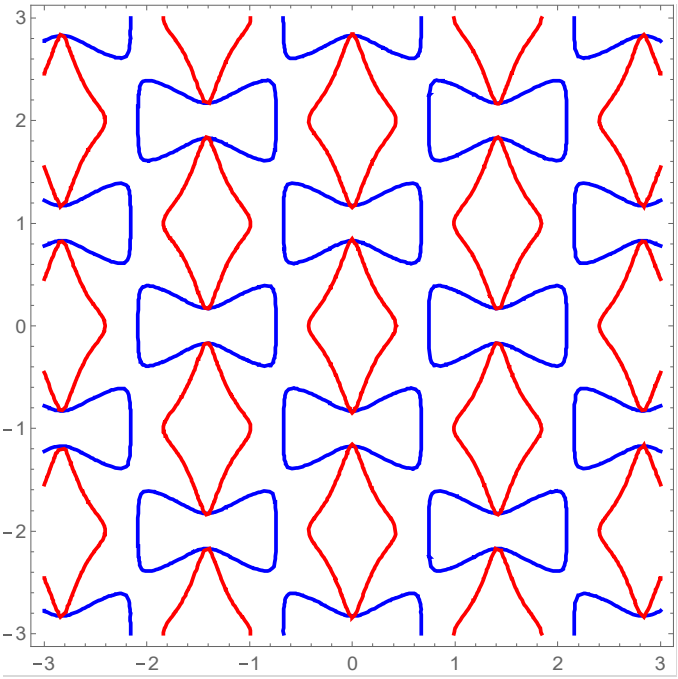

8. Open orbits and closed orbits in the (100) plane

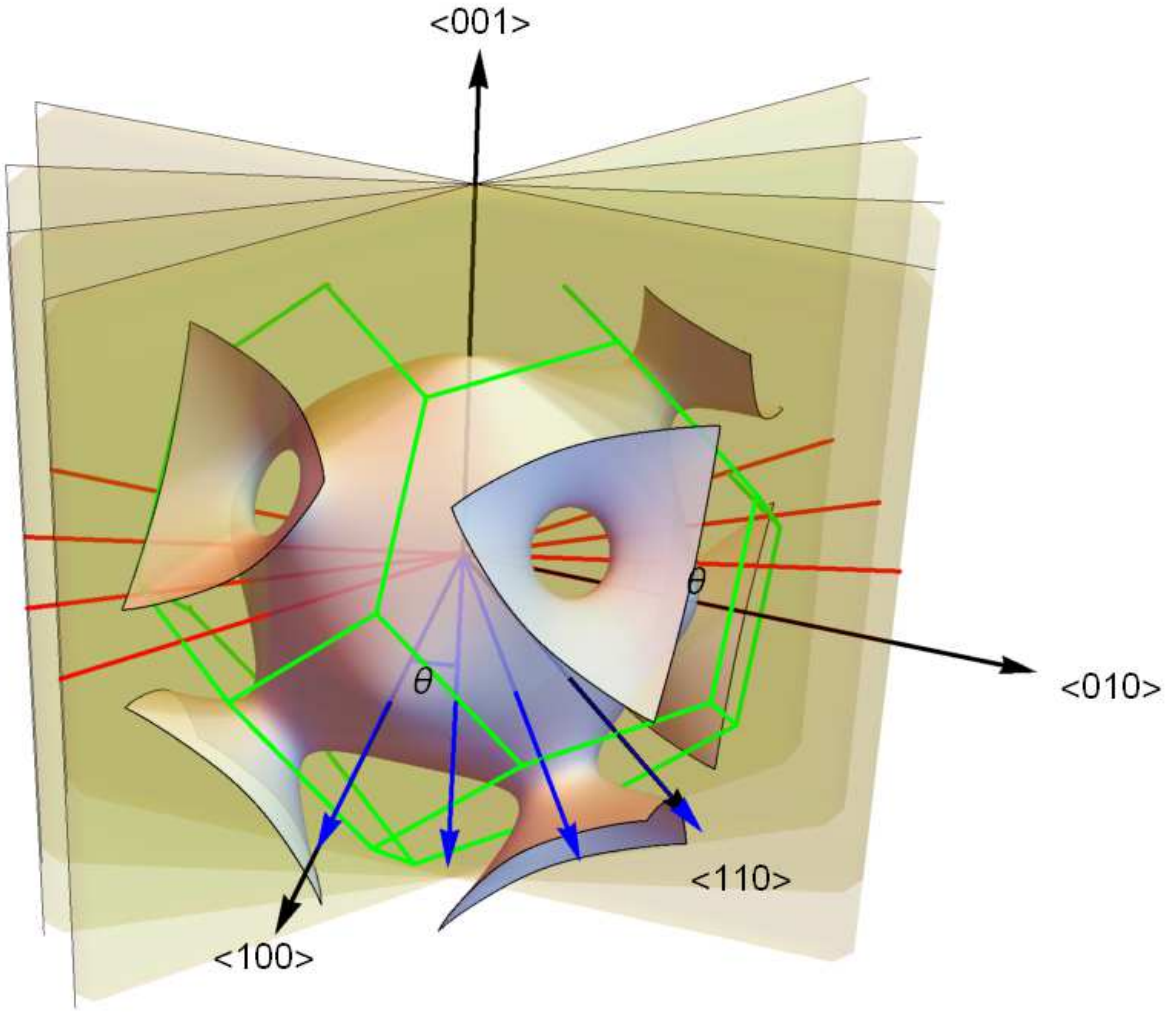

Open orbits and closed orbits for the plane including the directions <100>, <110},and <010>. θ is the rotation angle of the magnetic field direction around the <001> direction from the <100> axis.

$\theta = 0°$ for the <100> direction
$\theta = 45.0°$ for the <110> direction
$\theta = 90°$ for the <010> direction

We note that the vertical direction is the <001> direction in the following figures.

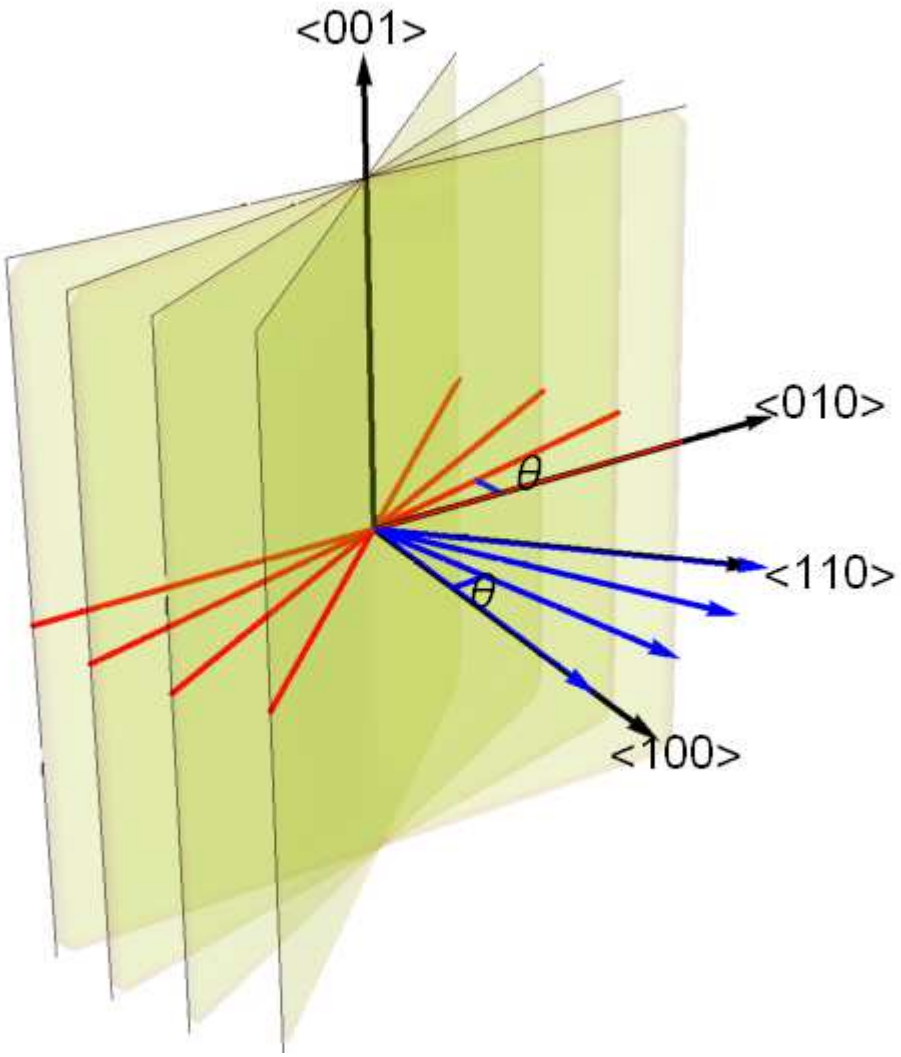

<100> direction

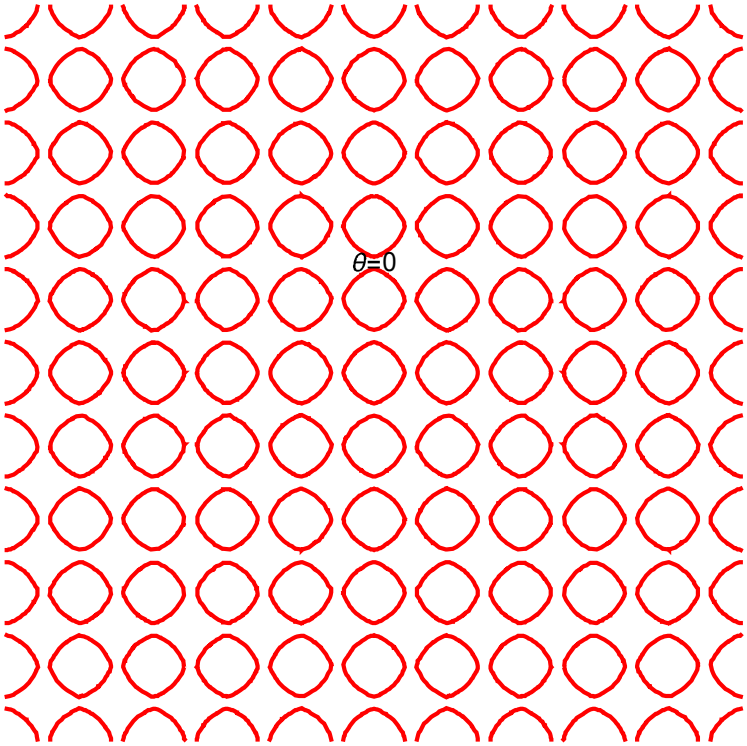
θ=0

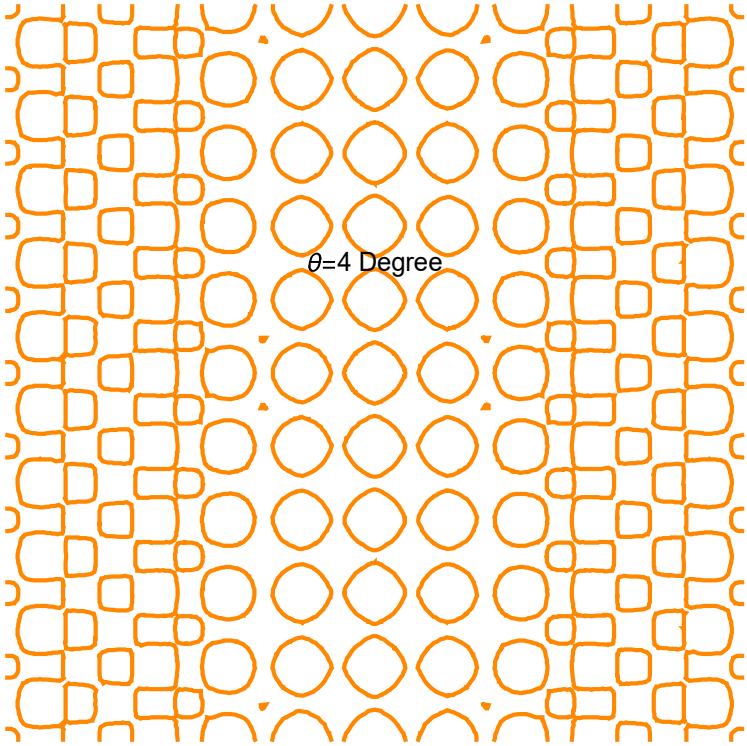
θ=4 Degree

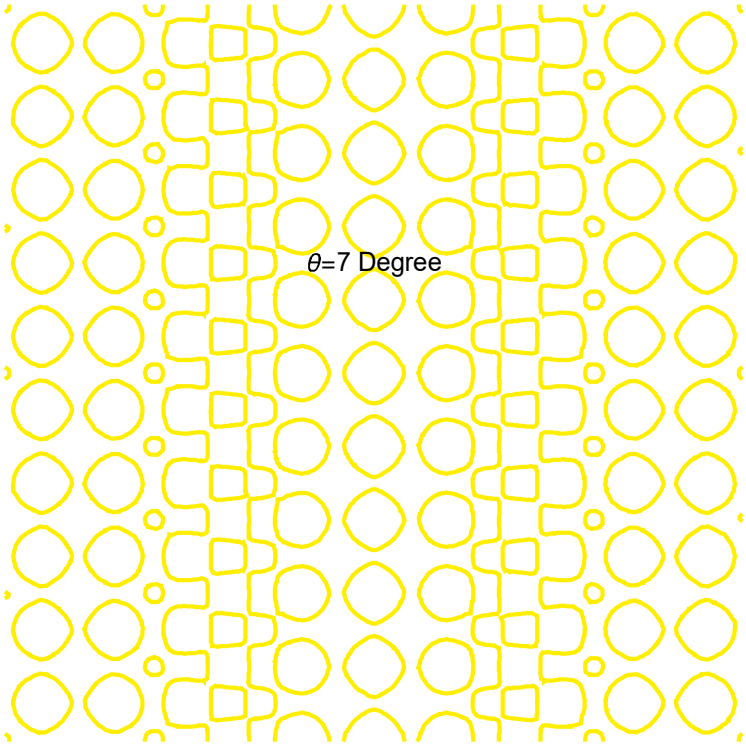

Aperiodic open orbits appear.

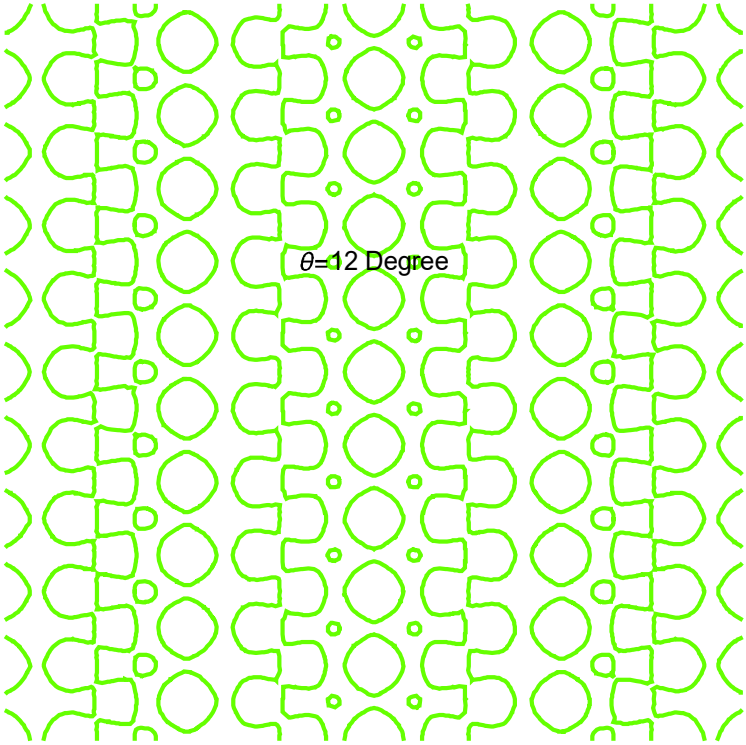

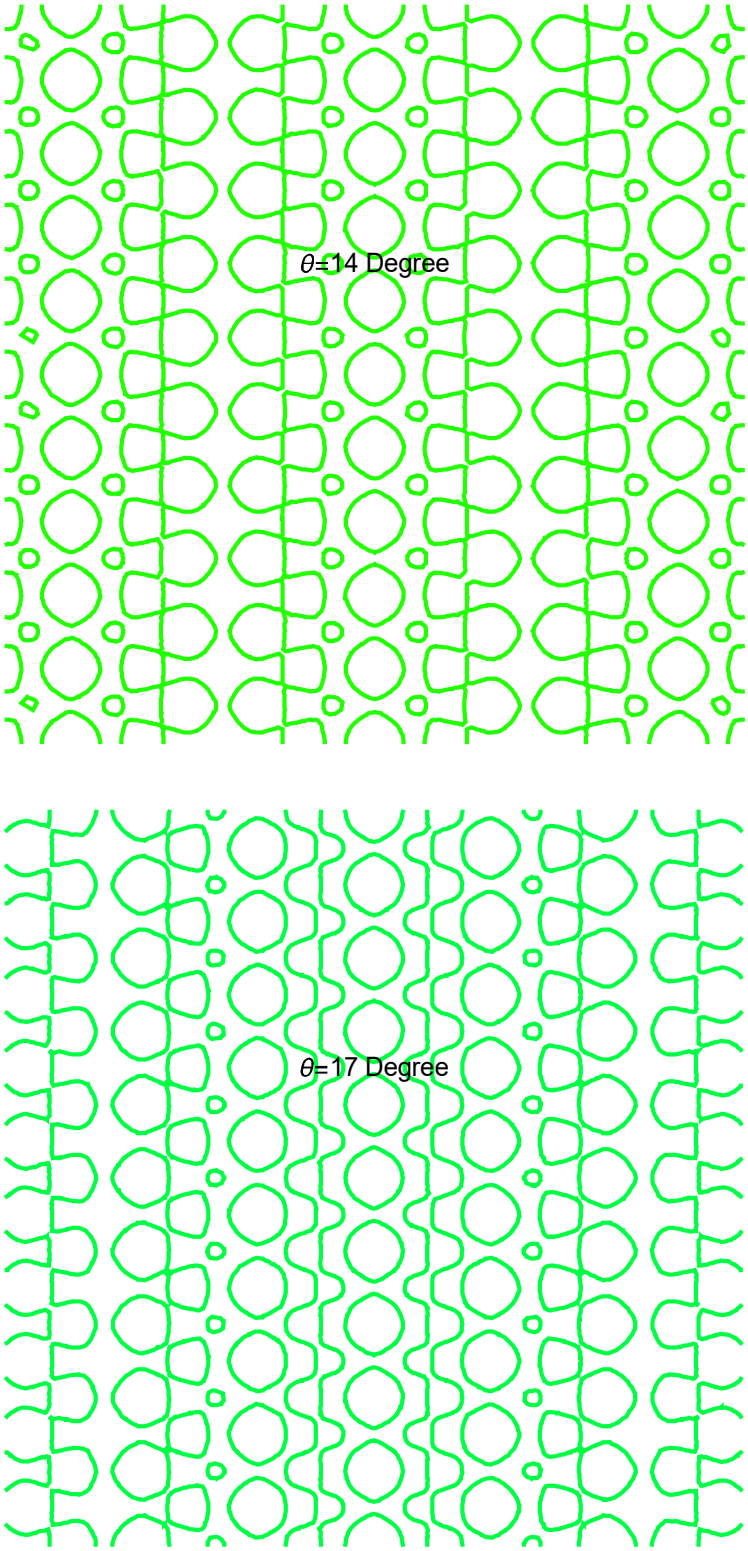

Periodic open orbits, as well as the closed orbits

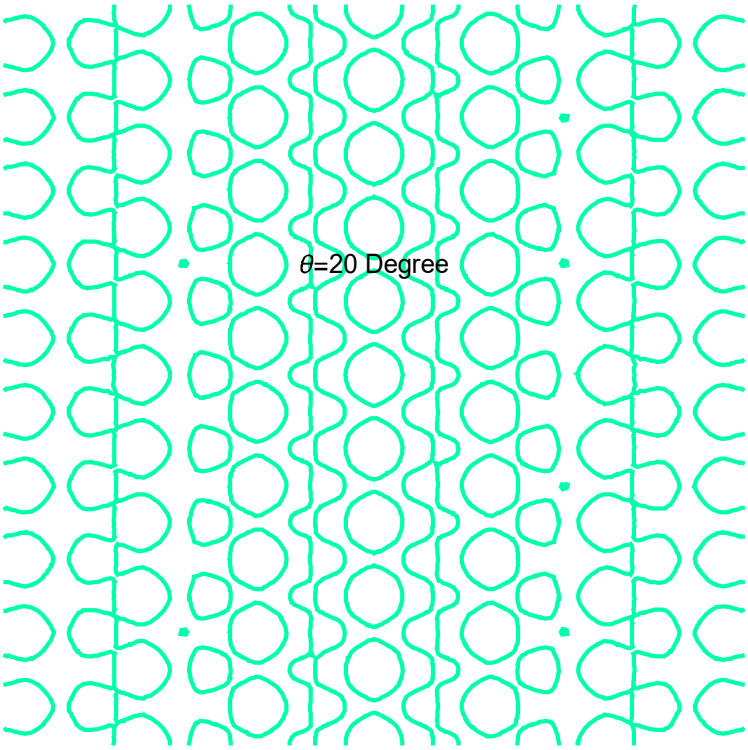
θ=20 Degree

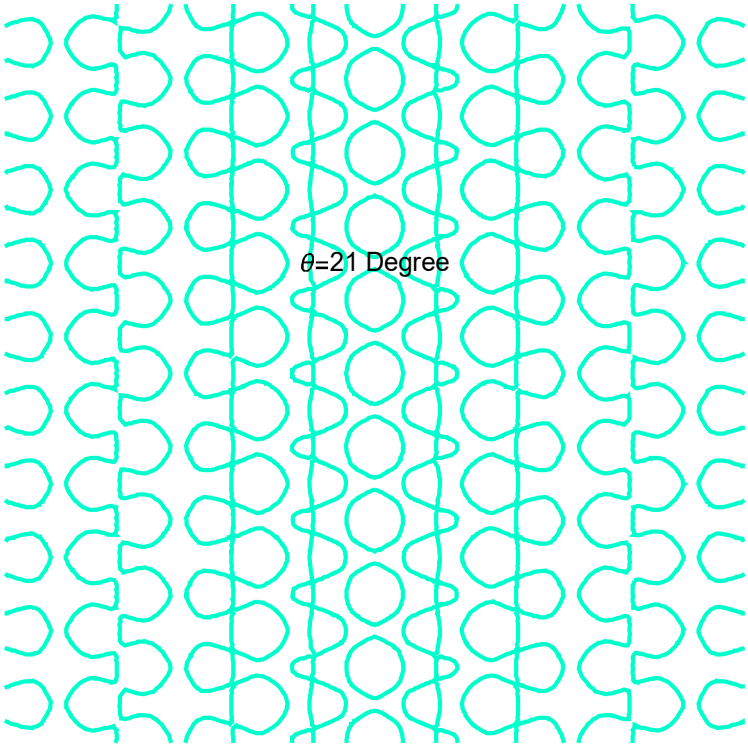
θ=21 Degree

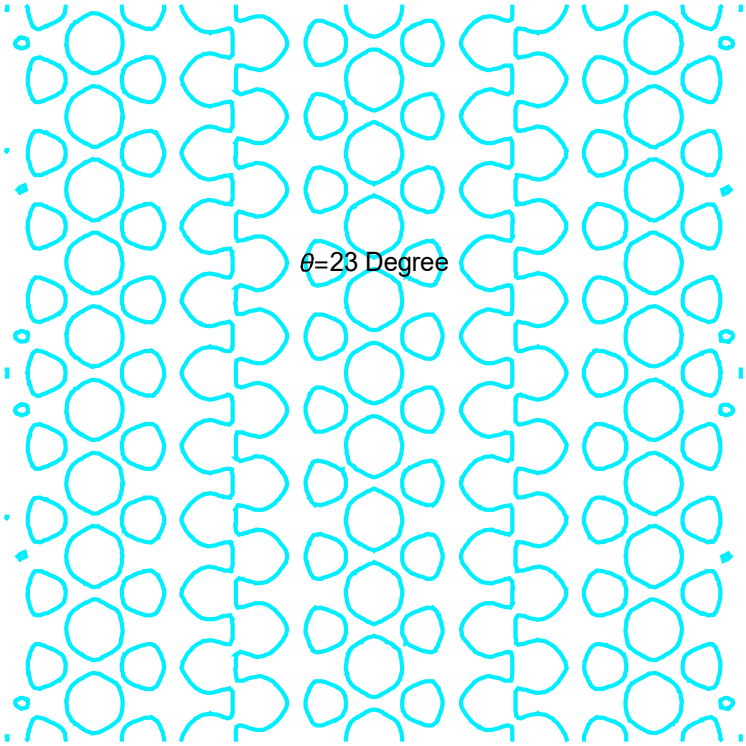

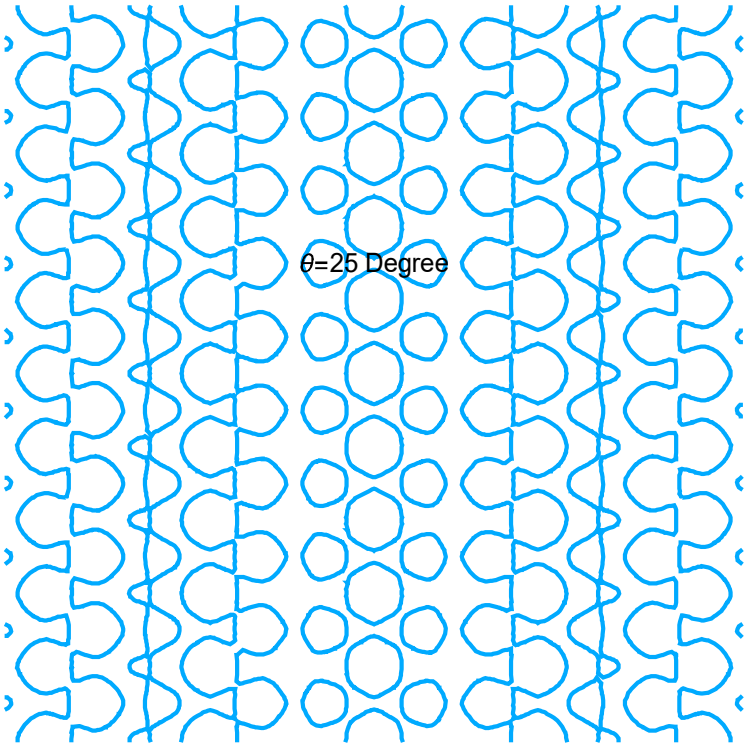

Periodic open orbits.

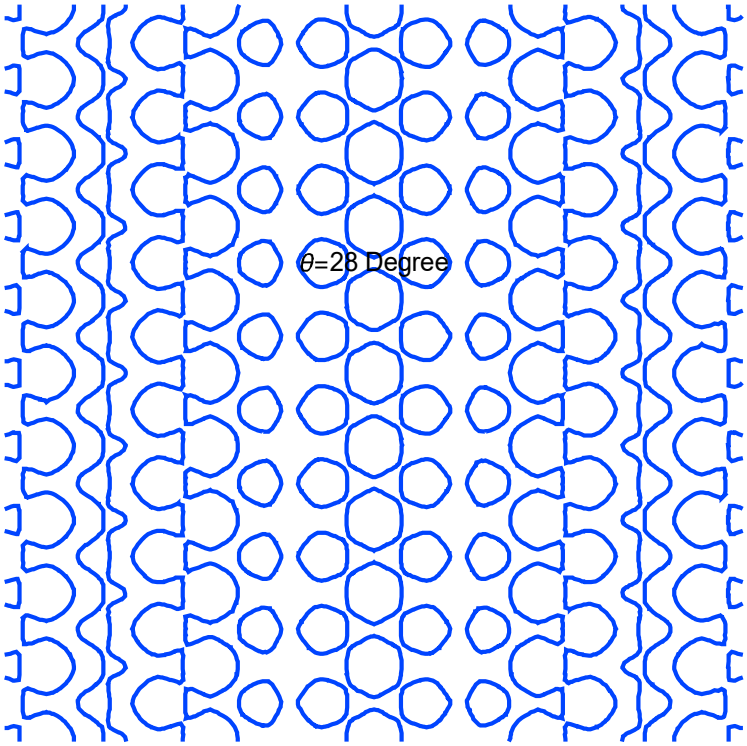

Closed orbits

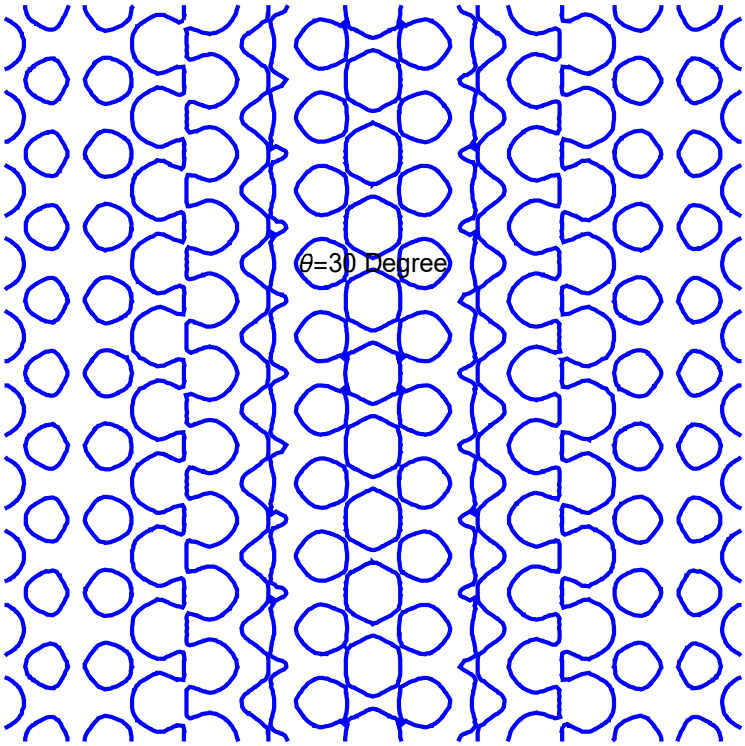

Aperiodic open orbits.

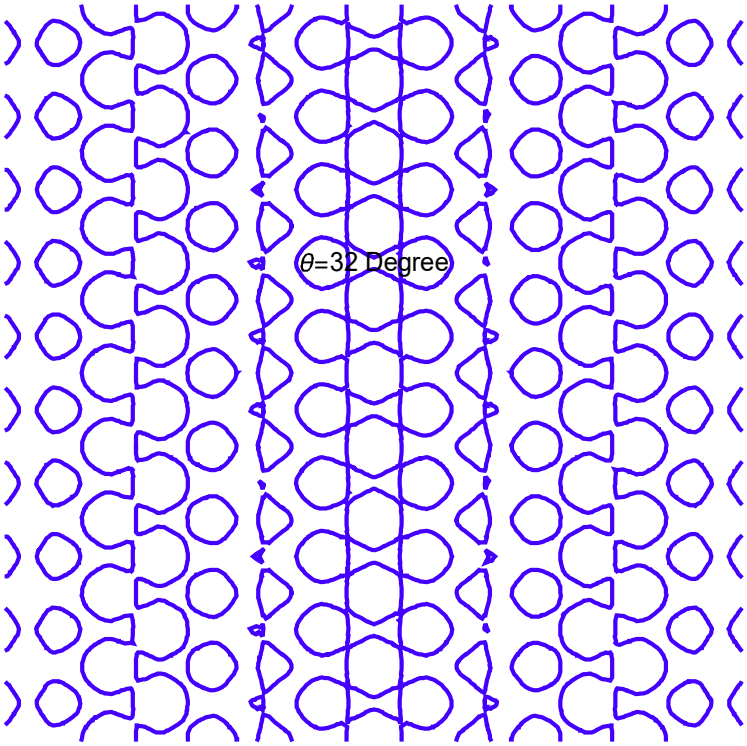

Closed orbits.

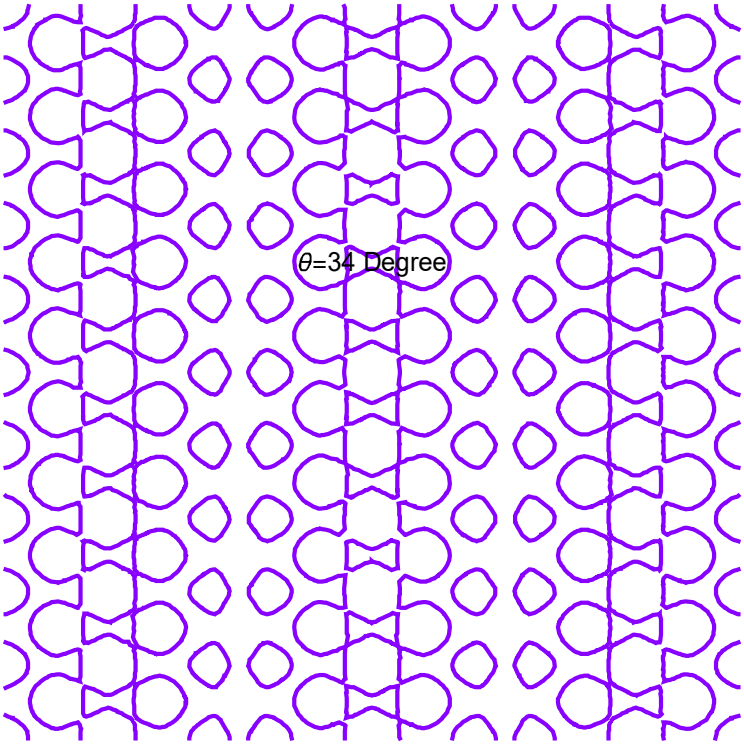

Periodic open orbits.

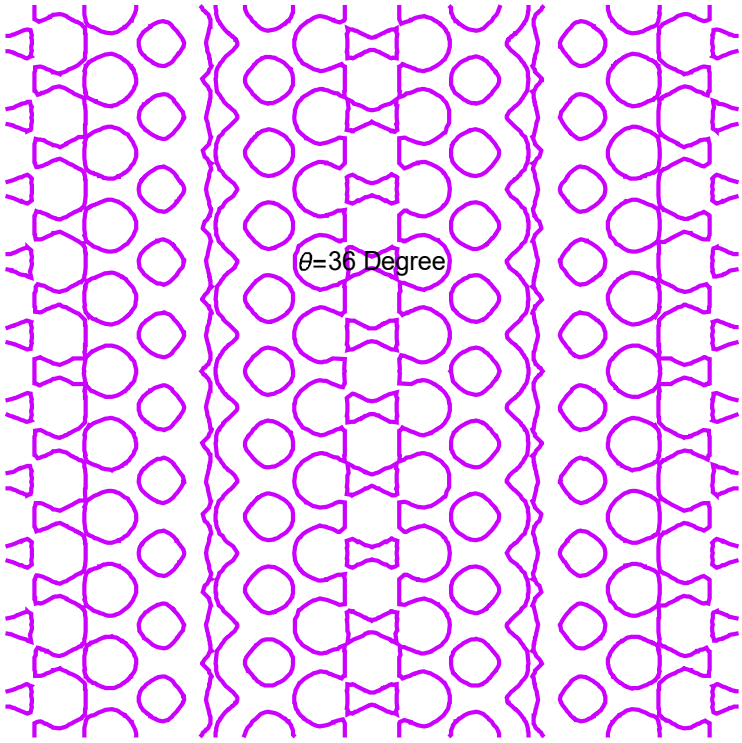
θ=36 Degree

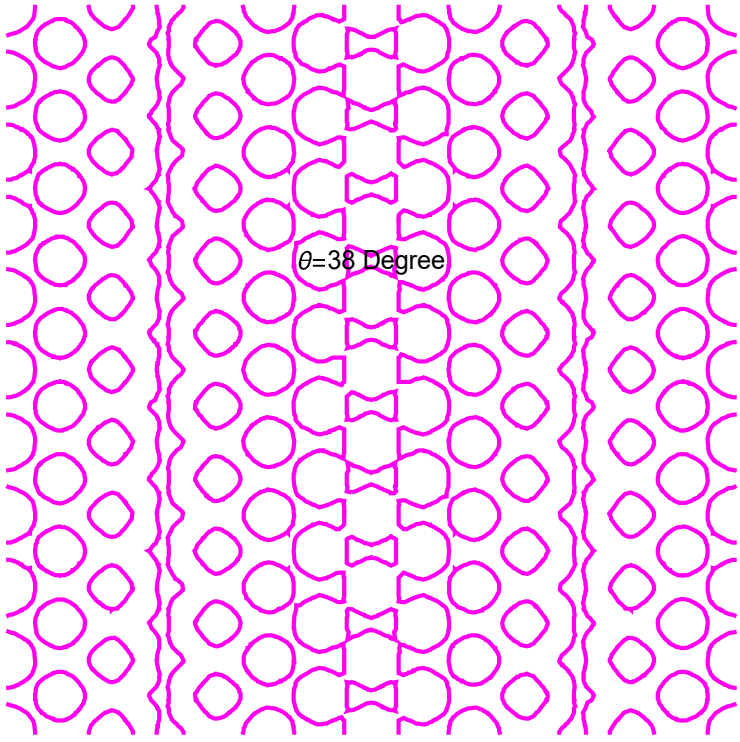
θ=38 Degree

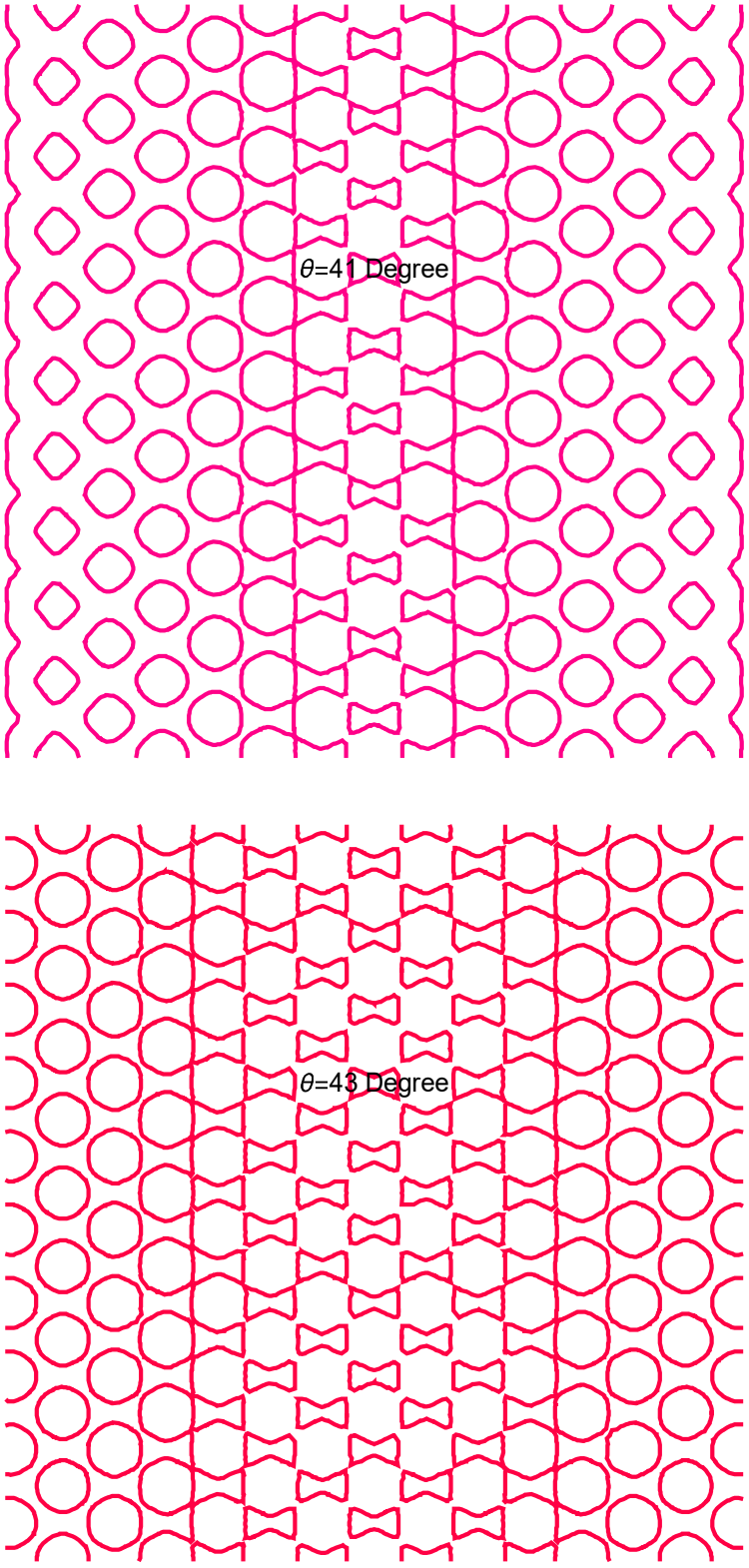

<110> direction

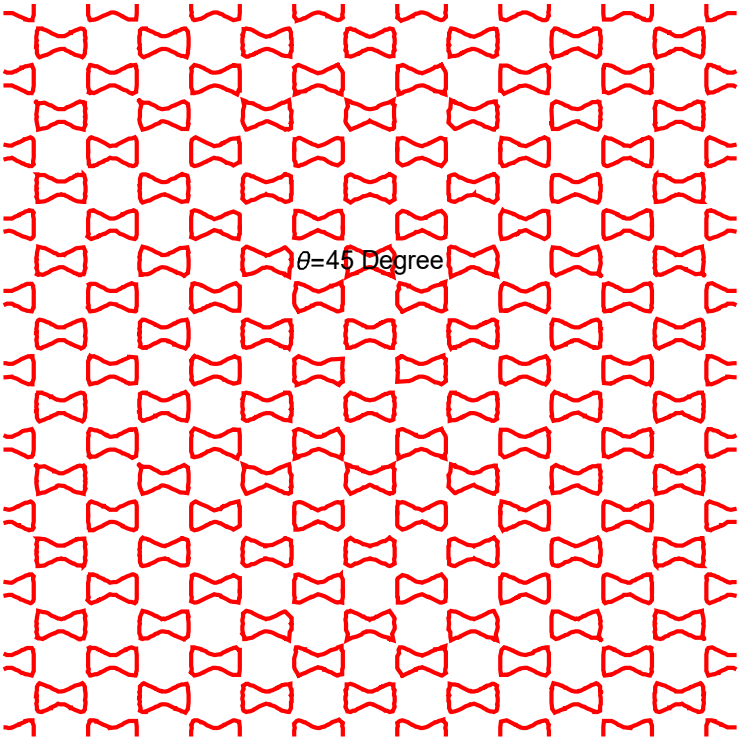

The dog’s boneappear.

9. Open orbits and closed orbit in the (110) plane

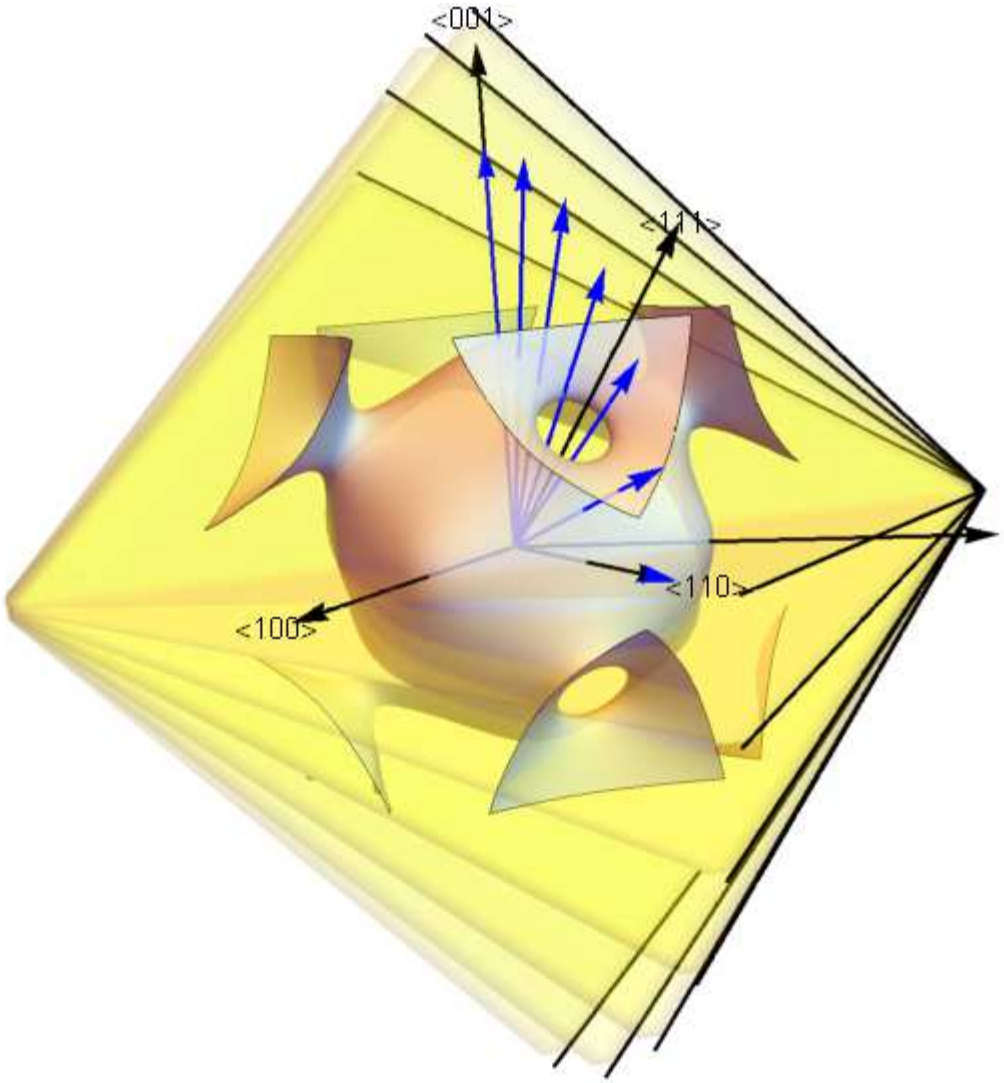

Open orbits and closed orbits for the plane including the directions <001>, <112}, <111>and <110>

θ is the rotation angle of the magnetic field direction from the <001> axis;

$\theta = 0°$ for the <001> direction
$\theta = 35.26°$ for the <112> direction
$\theta = 54.74°$ for the <111> direction
$\theta = 90°$ for the <110> direction

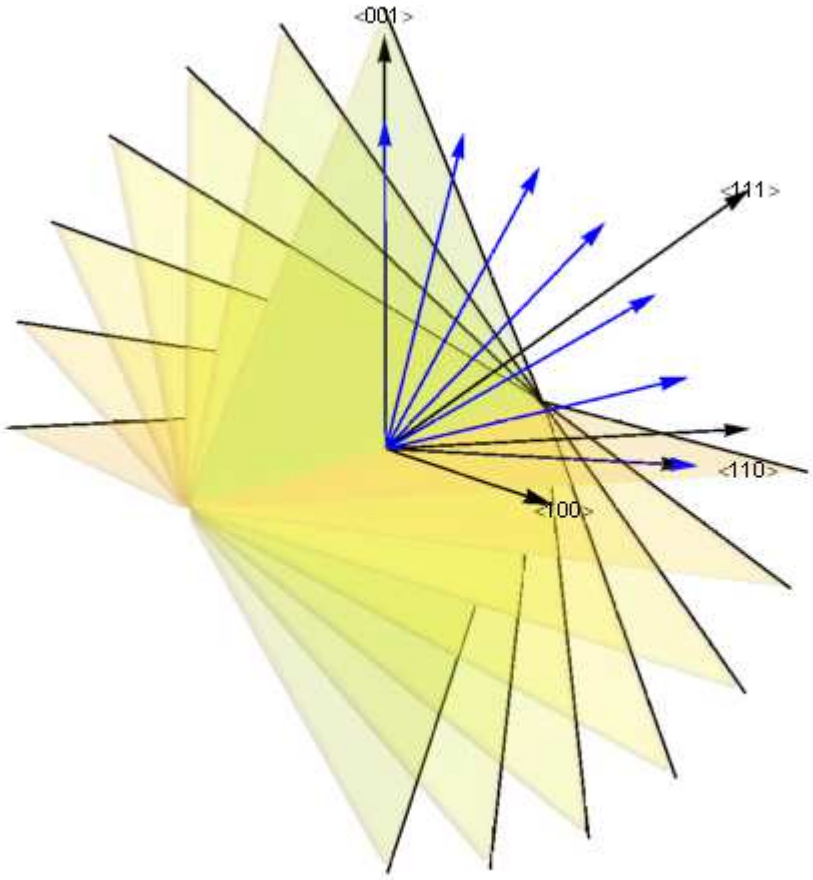

<001> directiom

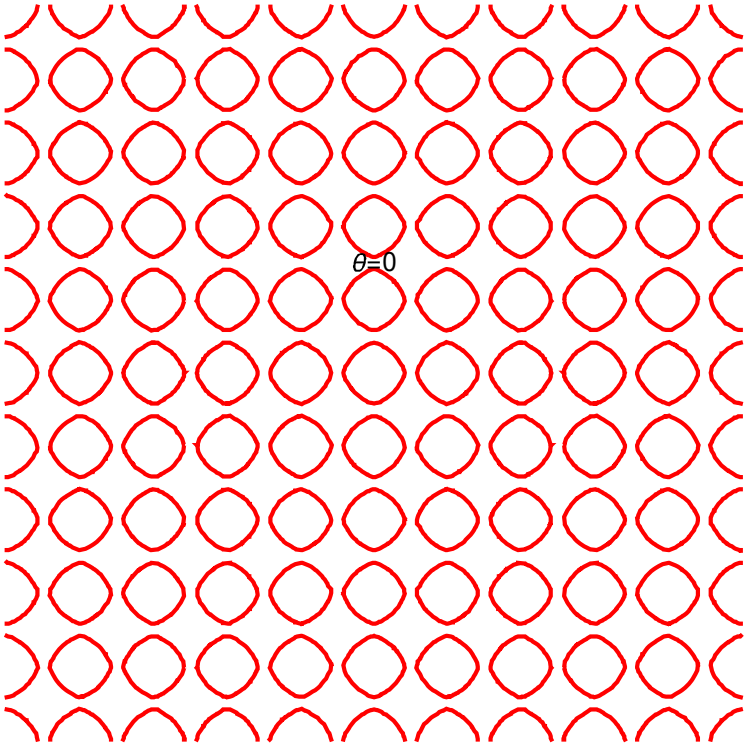
θ=0

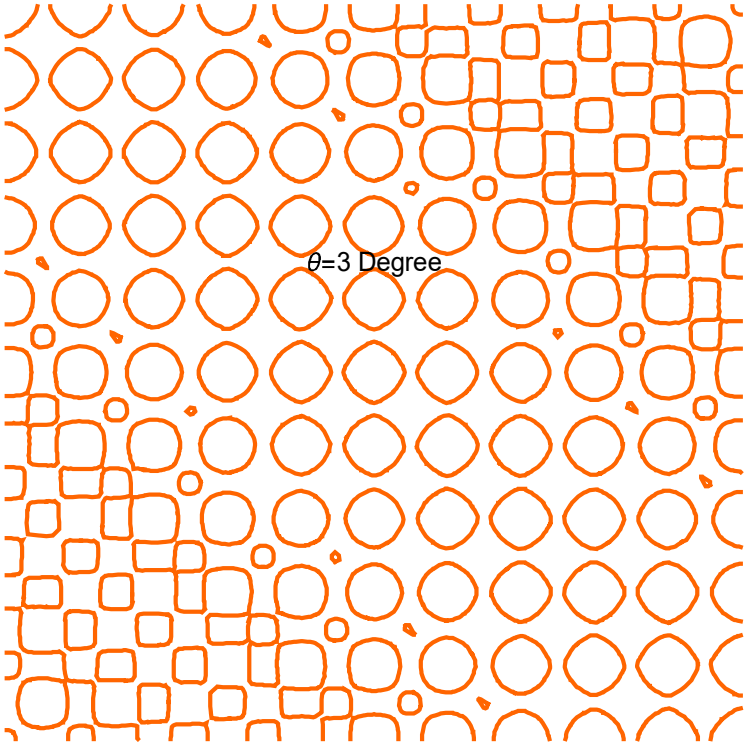
θ=3 Degree

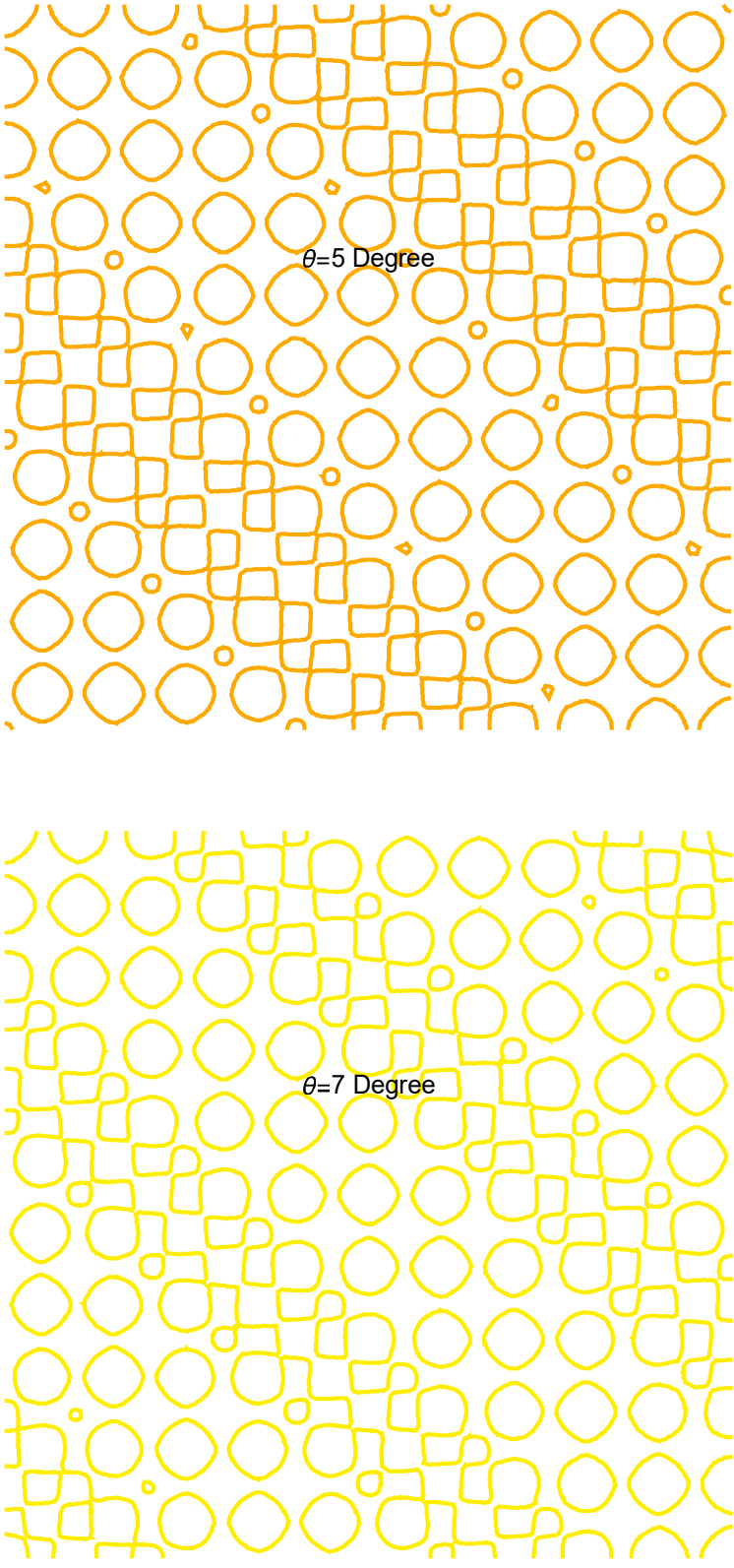

Aperiodic open orbit.

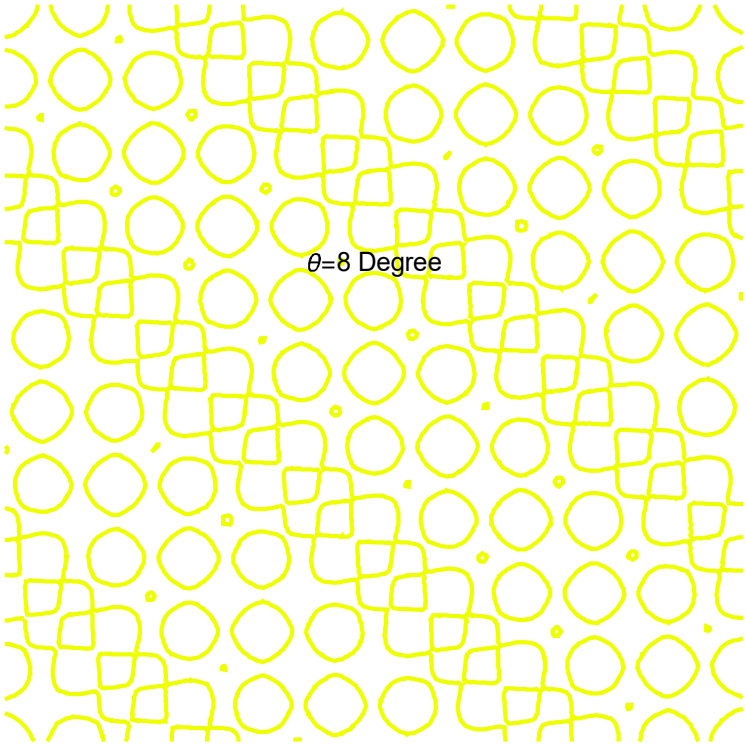
θ=8 Degree

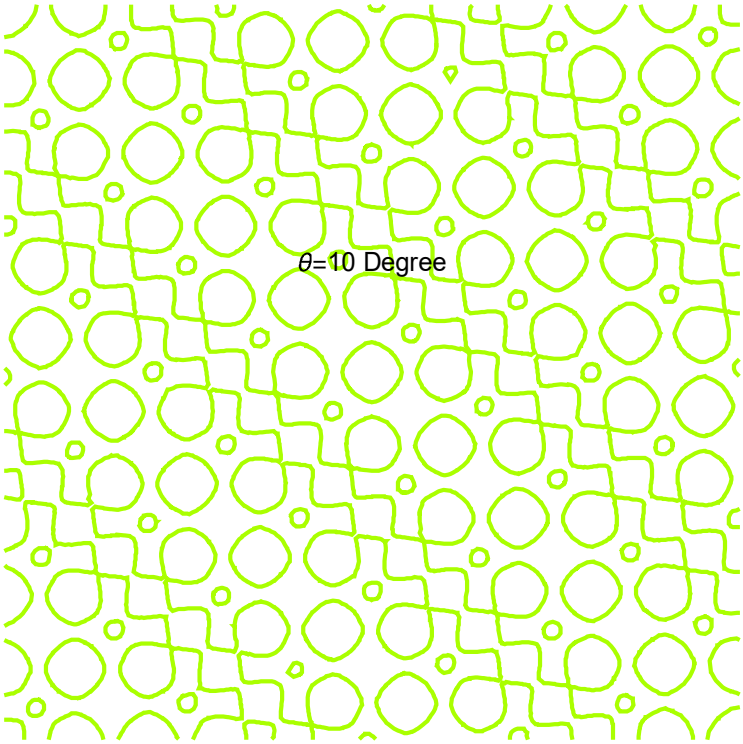
θ=10 Degree

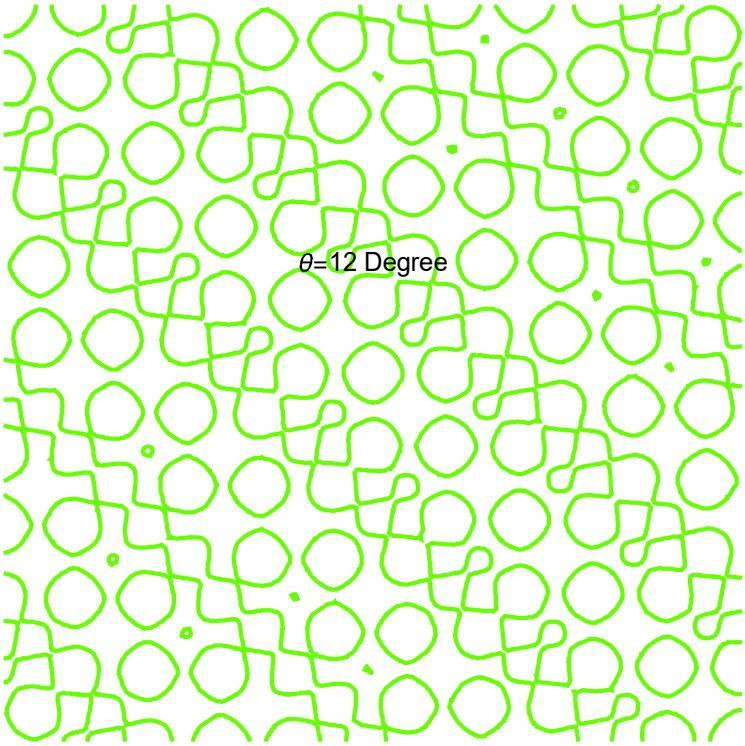
θ=12 Degree

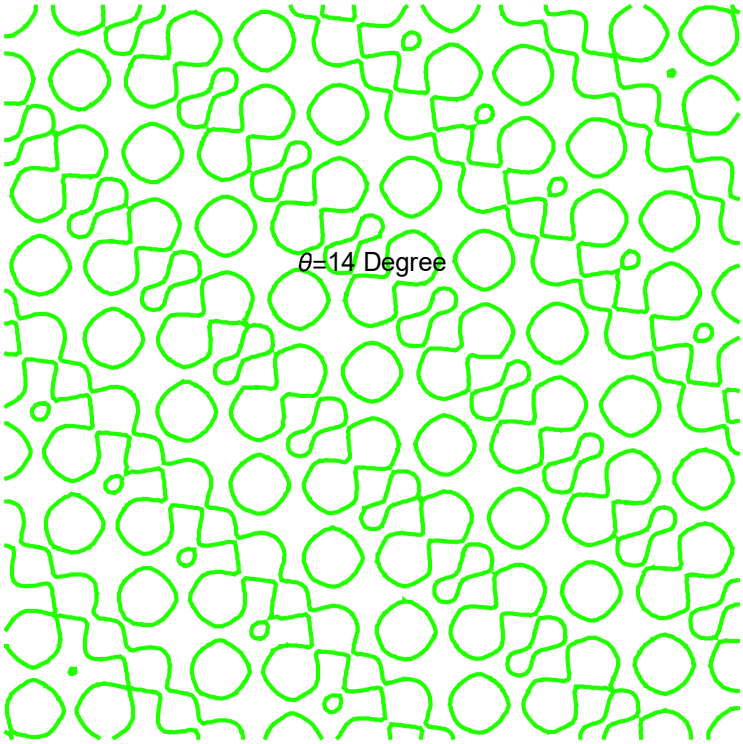
θ=14 Degree

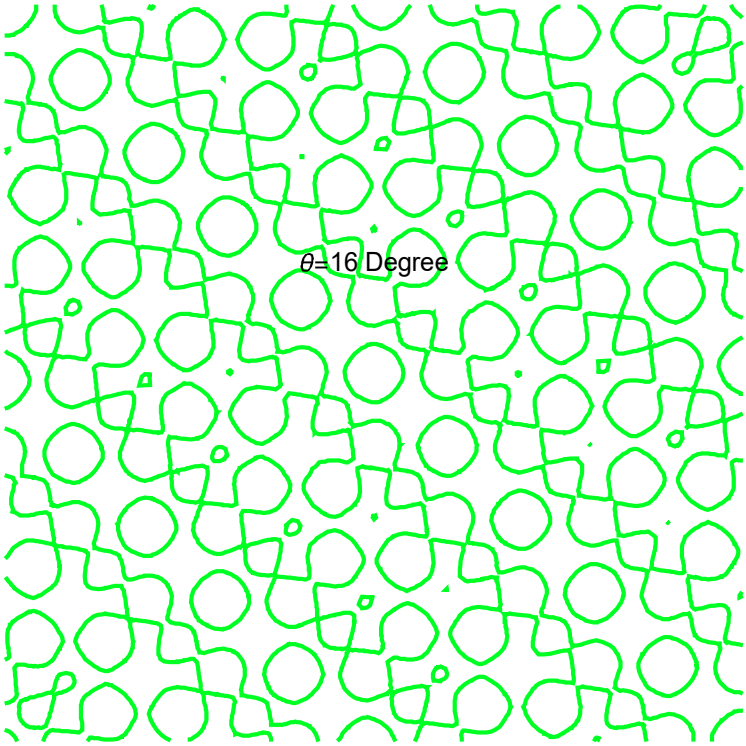

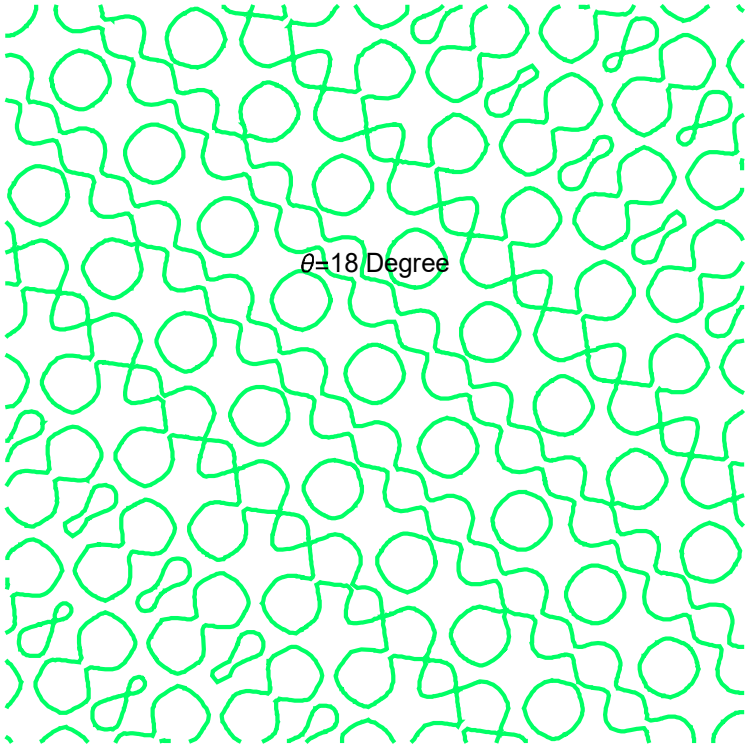

Periodic open orbits appear, in addition to the closed orbit for $\theta = 18°$.

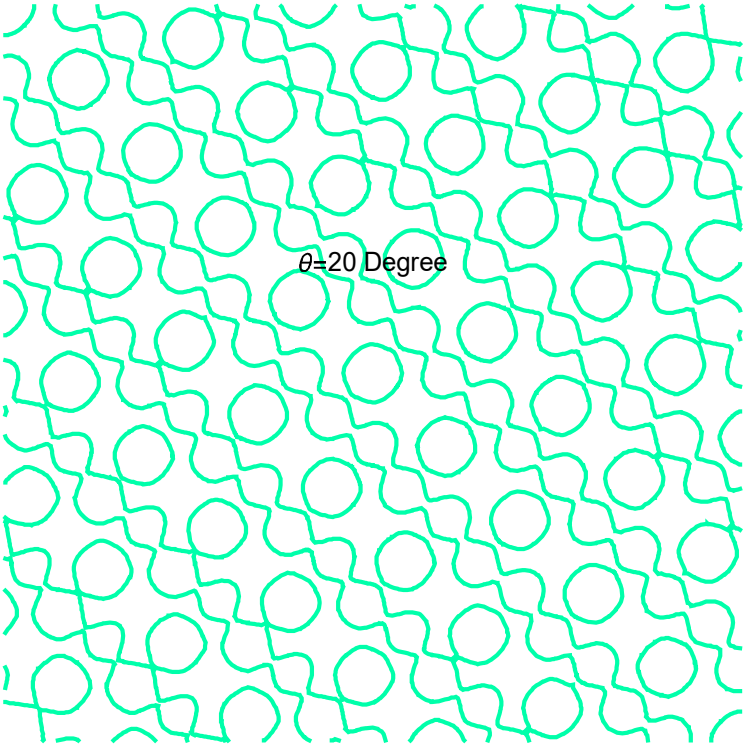
θ=20 Degree

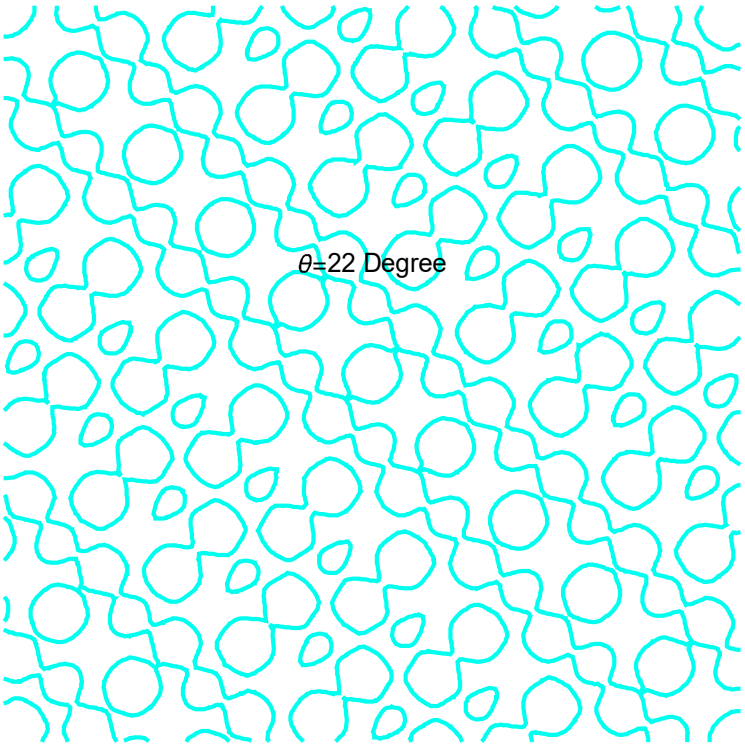
θ=22 Degree

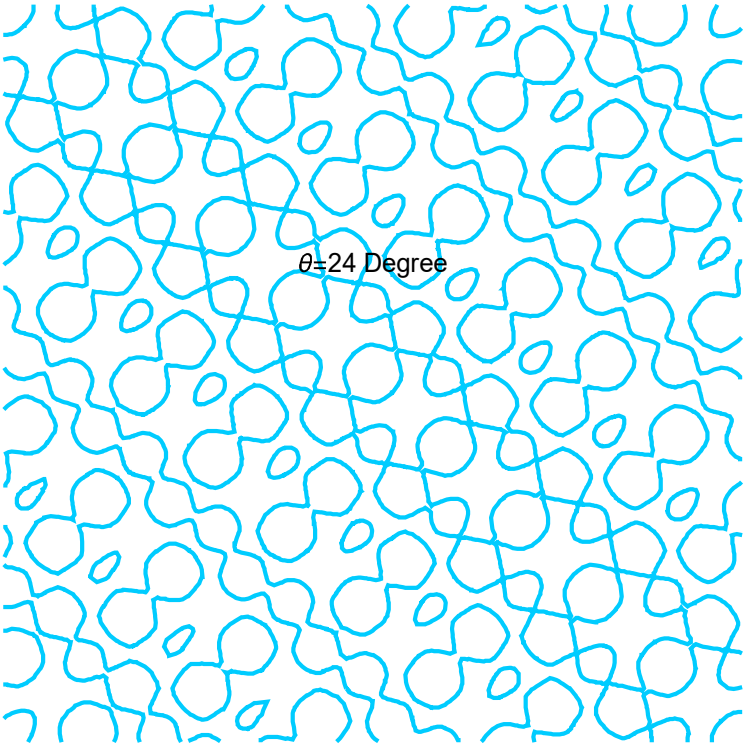
θ=24 Degree

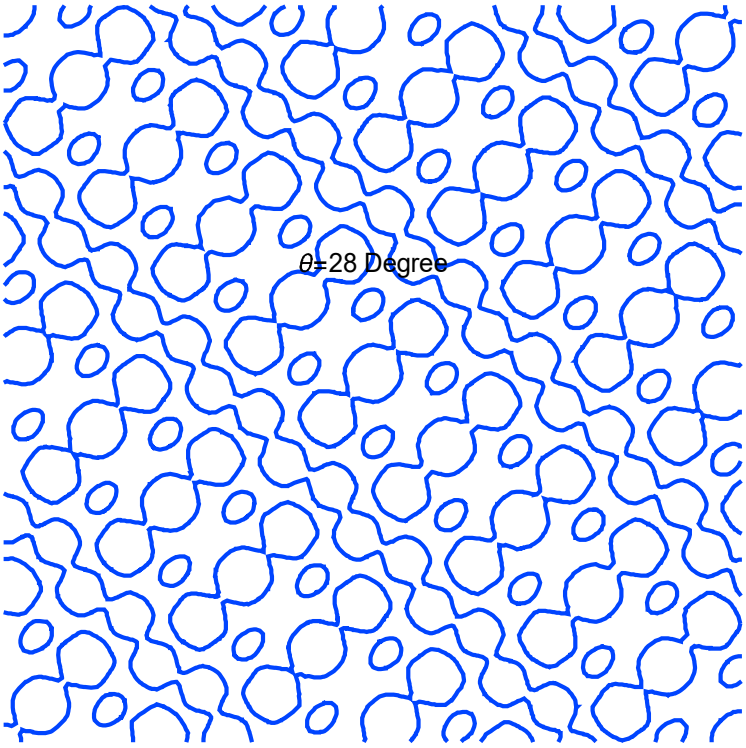
θ=28 Degree

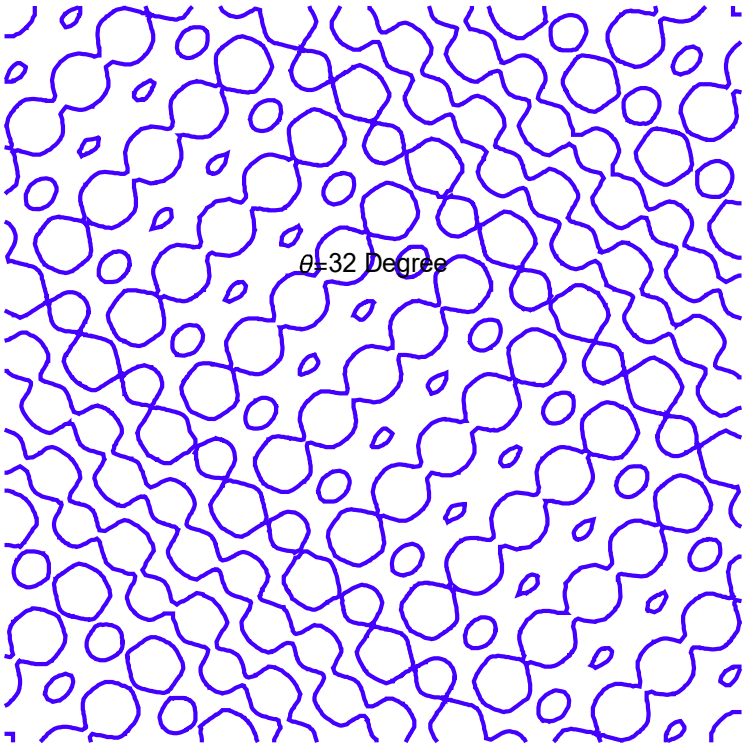

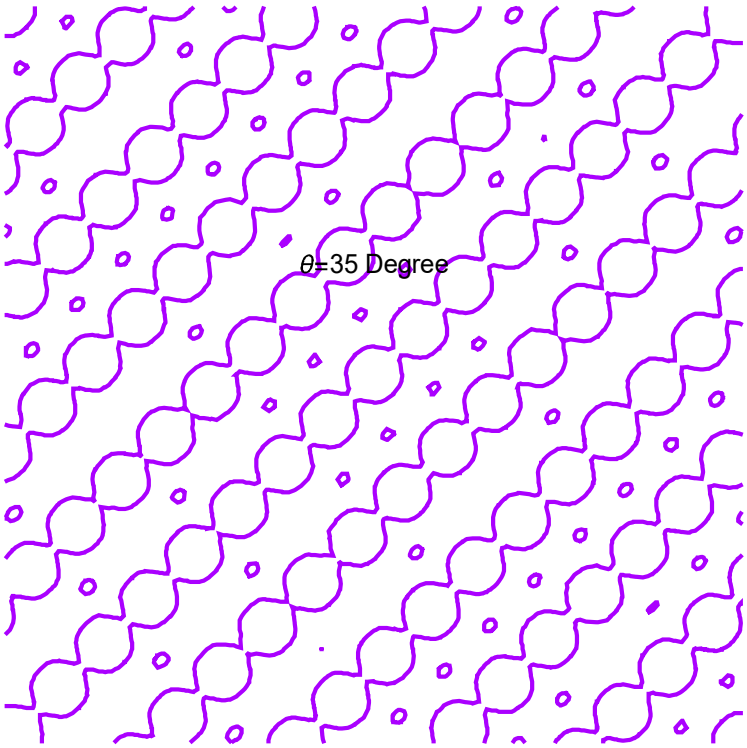

Periodic open orbits

θ=38 Degree

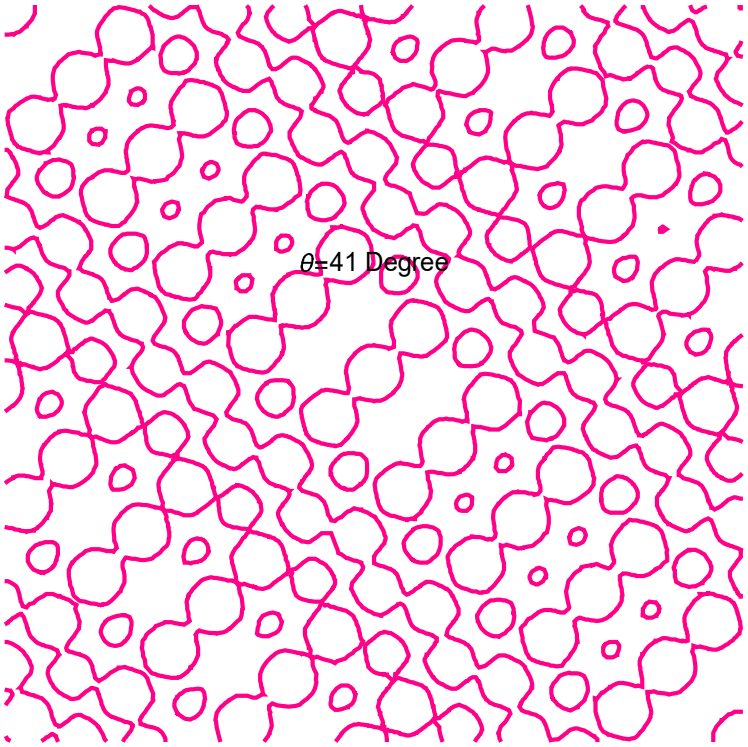
θ=41 Degree

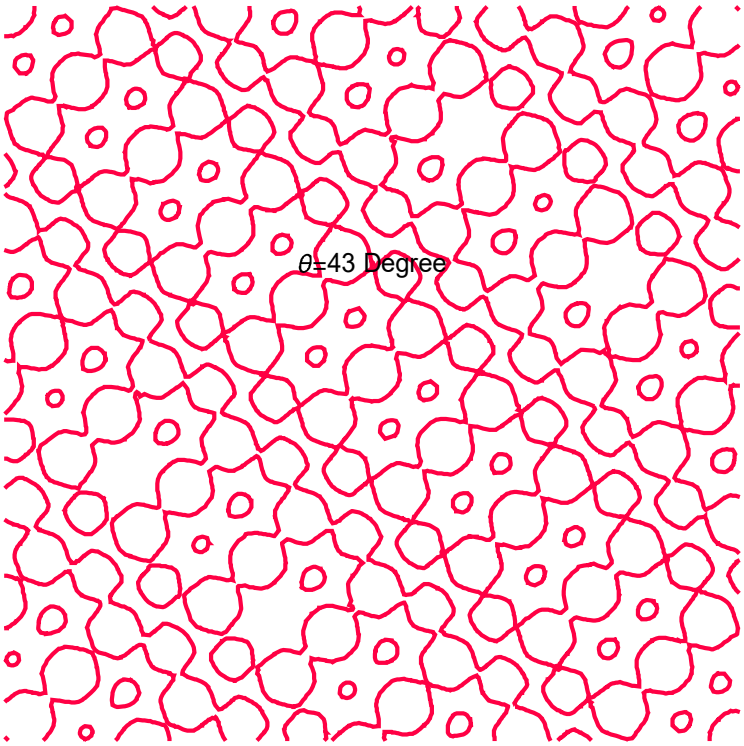

Aperiodic open orbits

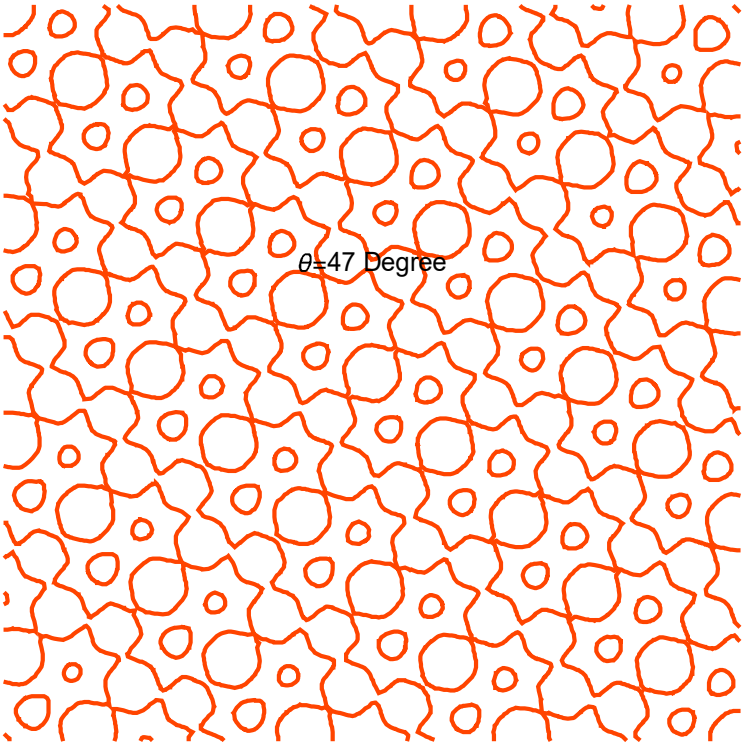

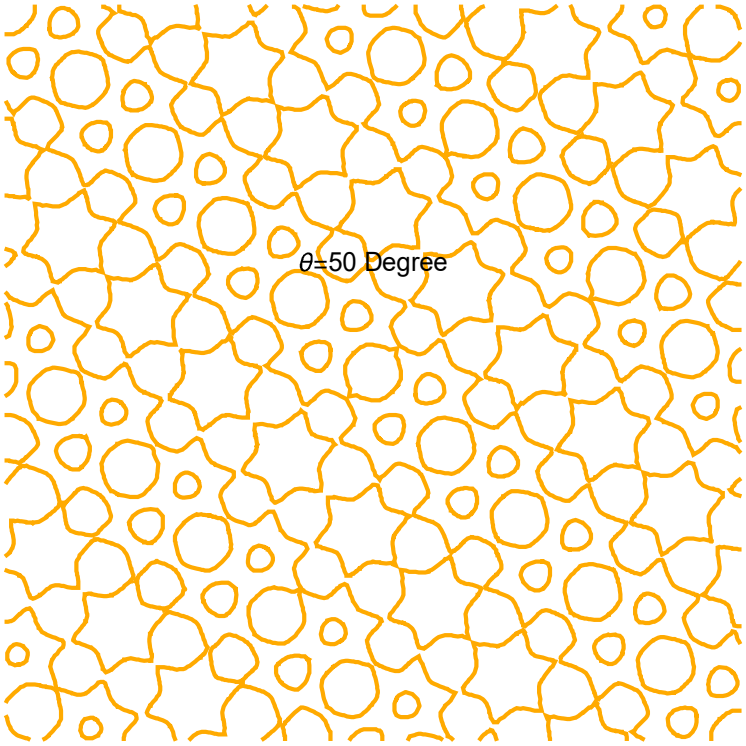
θ=50 Degree

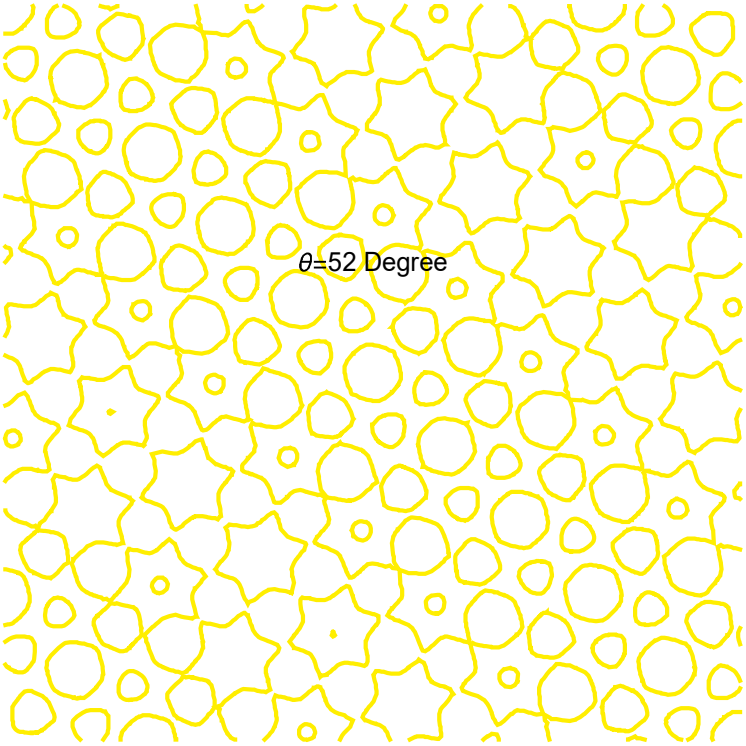
θ=52 Degree

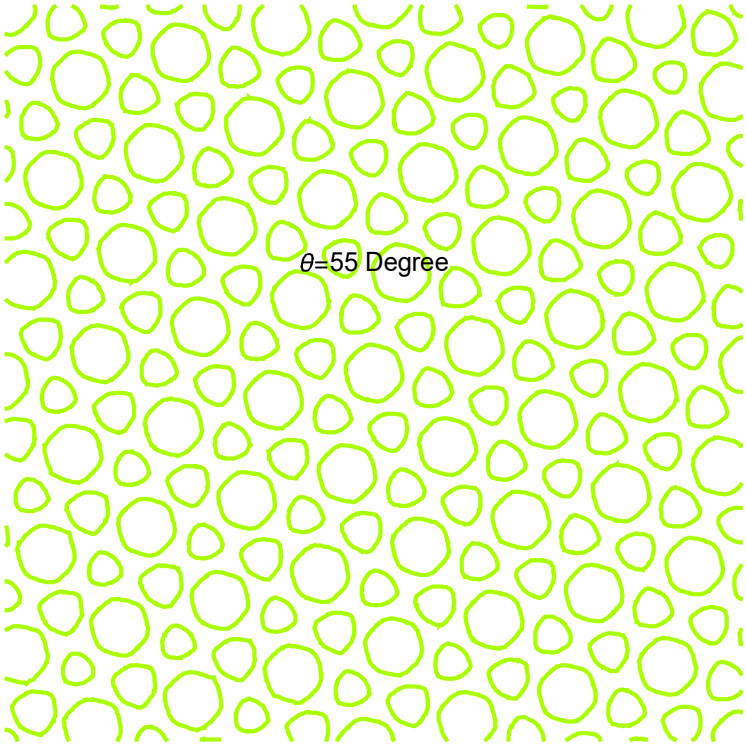

The direction <111>: $\theta = 54.636°$; The belly and neck orbits.

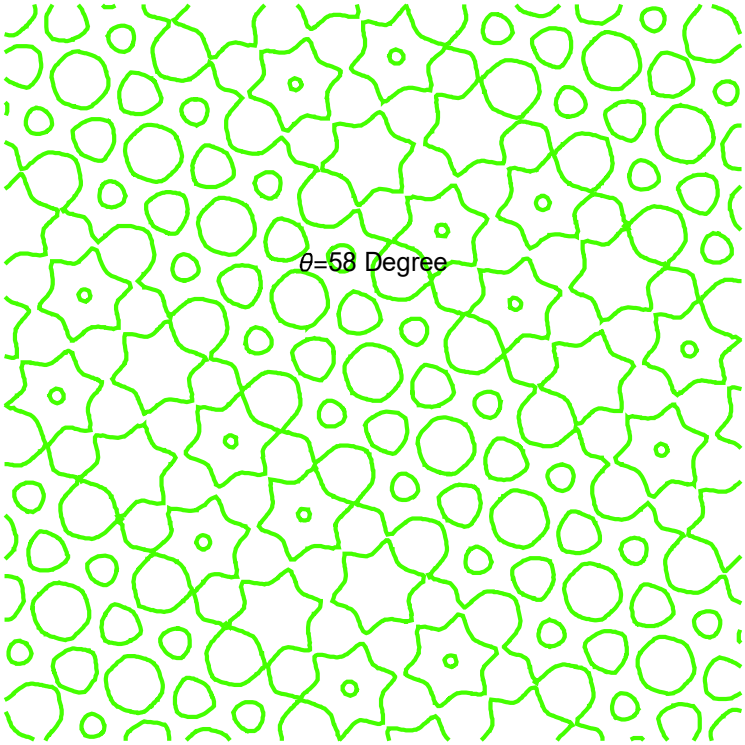

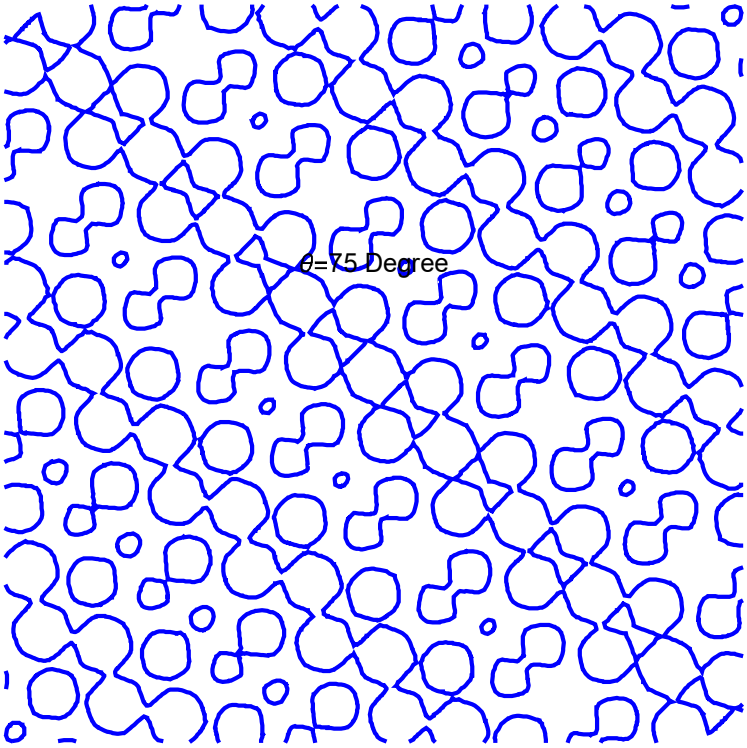
θ=75 Degree

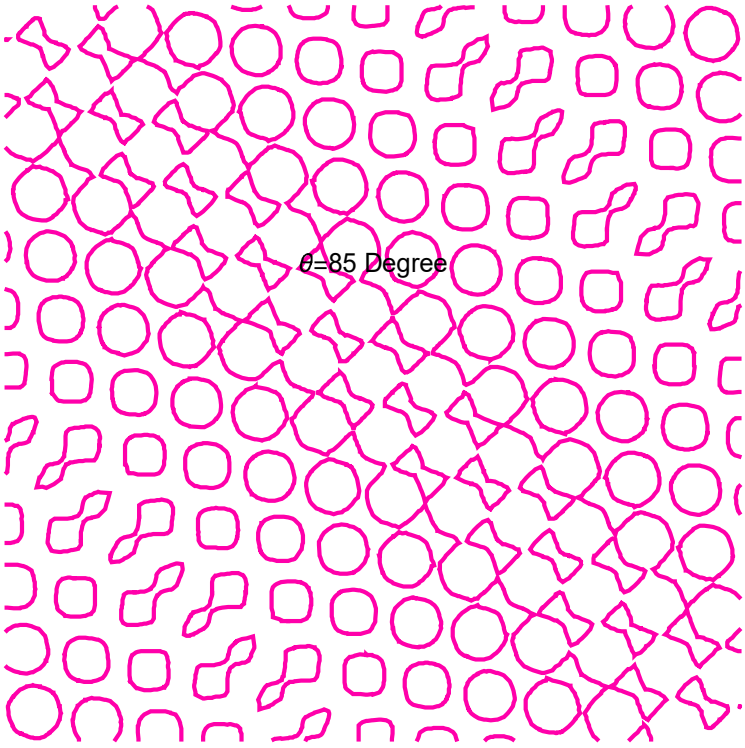
θ=85 Degree

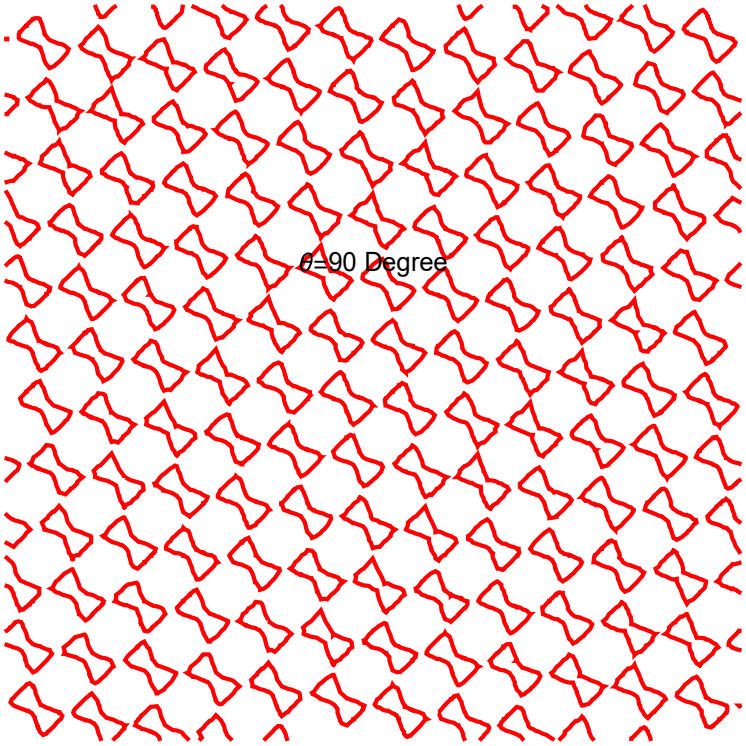

<110> direction: the dog's bone orbit.

10. Open orbits and magnetoresistance

It well known that the transverse magnetoresistance shows a different field dependence. It increses with B^2 when the Fermi surface suppots the existence of open orbit normal to the field direction. This phenomenon can be used to determine the existence of open orbits from the experiments of the transverse magnetioresistance at the fixed magnitude of the magnetic field as a function of the field direction. Note that the magnitude of the magnetoresistance takes a local maximum for the open orbits in the plane normal the field direction, and takes local minumum for the closed orbits in the plane normal to the field direction.

Here we show two experimental results, one for Cu and the other for Au. It is a little surprising for us that these data were taken in 1950's – 60's. We could not find any data after 1980's, as far as we know.

Cu

The transverse magnetoresistance of Cu as a function of field directions where the magnetic field is rotated in the (100) plane, including the field directions of <100>, <110>, and <010>.

J.R. Klauder, W.A. Reed, C.F. Brenner, and J.E. Kunzler, Phys. Rev. 141, 592 (1966).

$\theta = 74°$ from the <001> direction; $\phi = 90° - \theta = 16°$ from the <110> direction.

There is an open orbit, which causes the large amount of magnetiresistance for Au. Here we assume that the Fermi surface of Au is similar to that of Cu

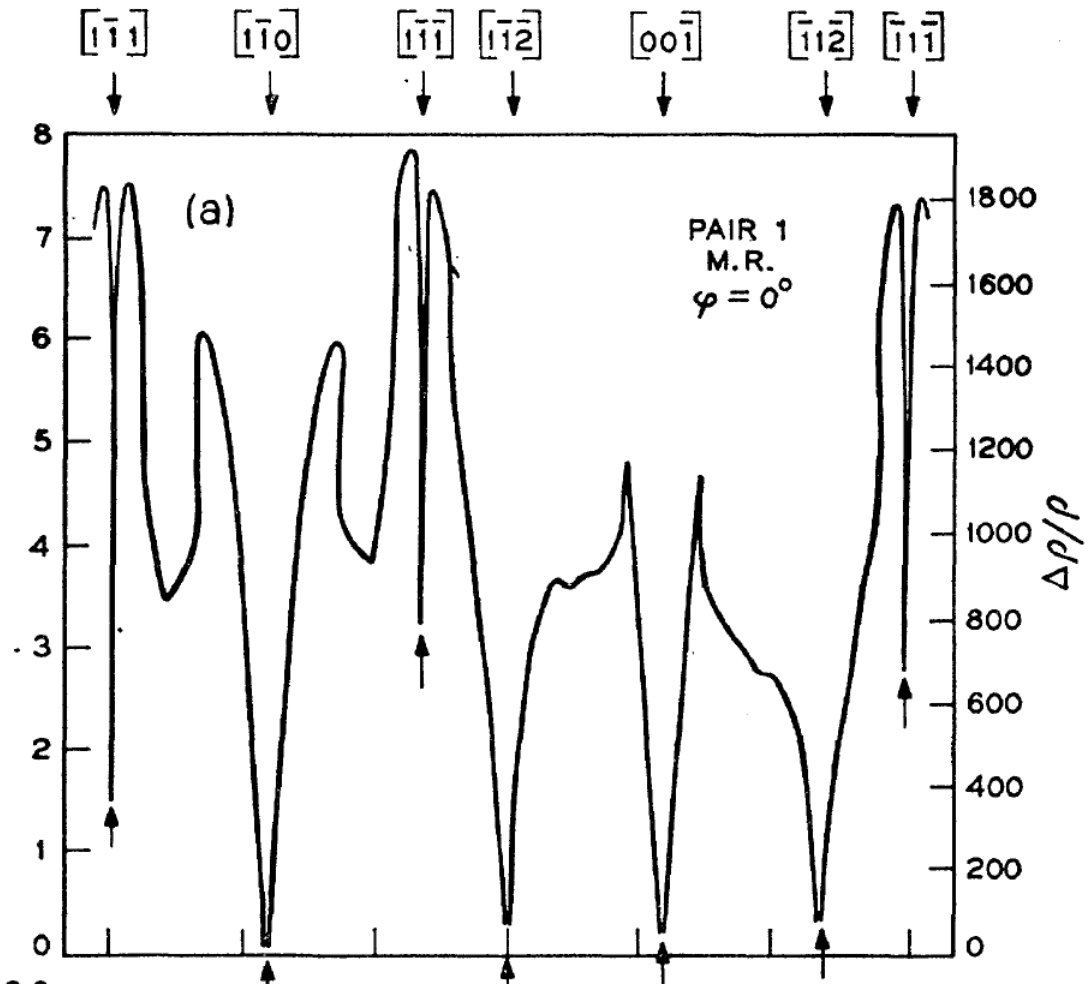

Fig. Variation of high-field transverse magnetoresistance in Cu as *B* is rotated in the (110) plane. The current is along the <110>.

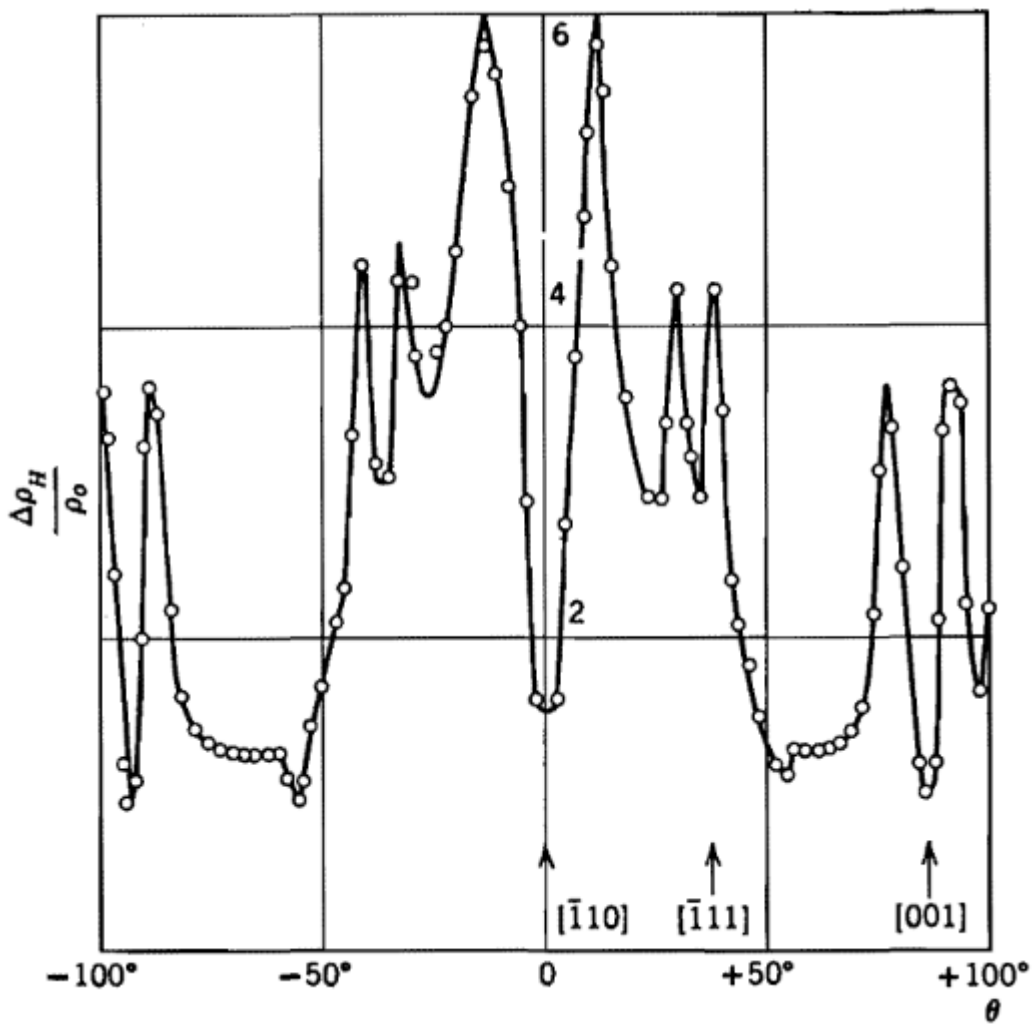

Fig. Variation of trnsverse magnetoresistance with field direction in a field of 23.5 kOe, for a single crystal Au specimen with current // [110](Gaidukov, 1959).

$\theta = 78°$ from the <001> direction; $\phi = 90° - \theta = 12°$ from the <110> direction.

There is an open orbit, which causes the large amount of magnetiresistance for Au. Here we assume that the Fermi surface of Au is similar to that of Cu

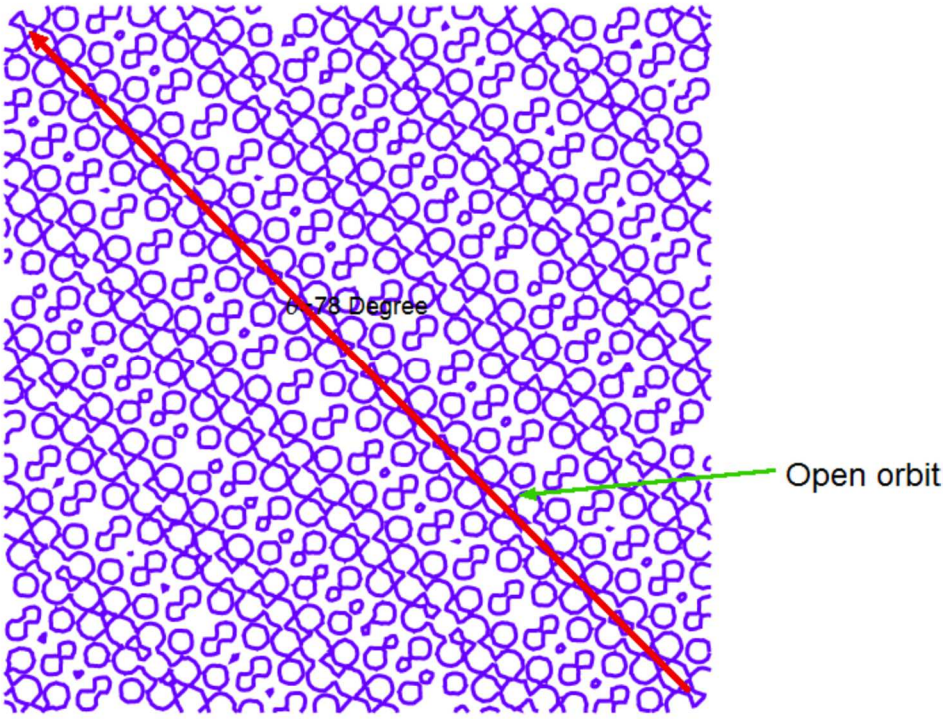

FFT pattern

<001> direction

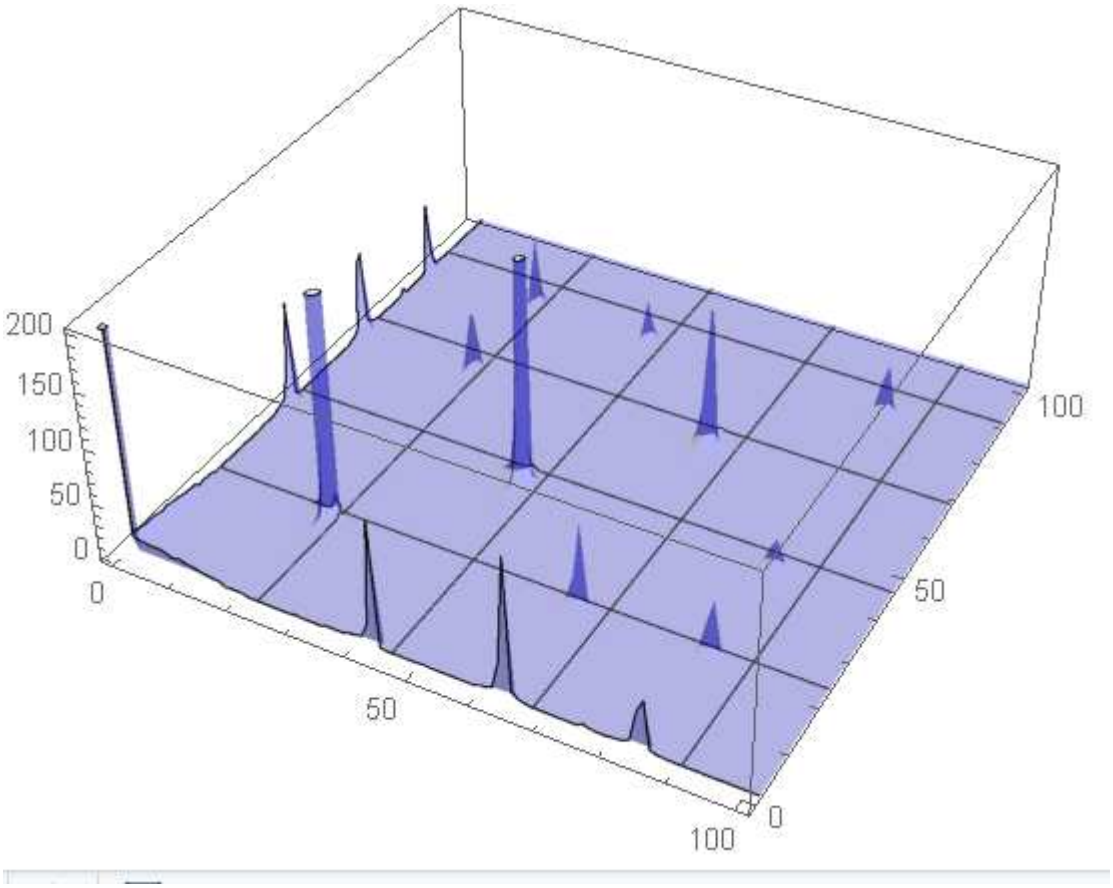

$\theta = 78^{\circ}$

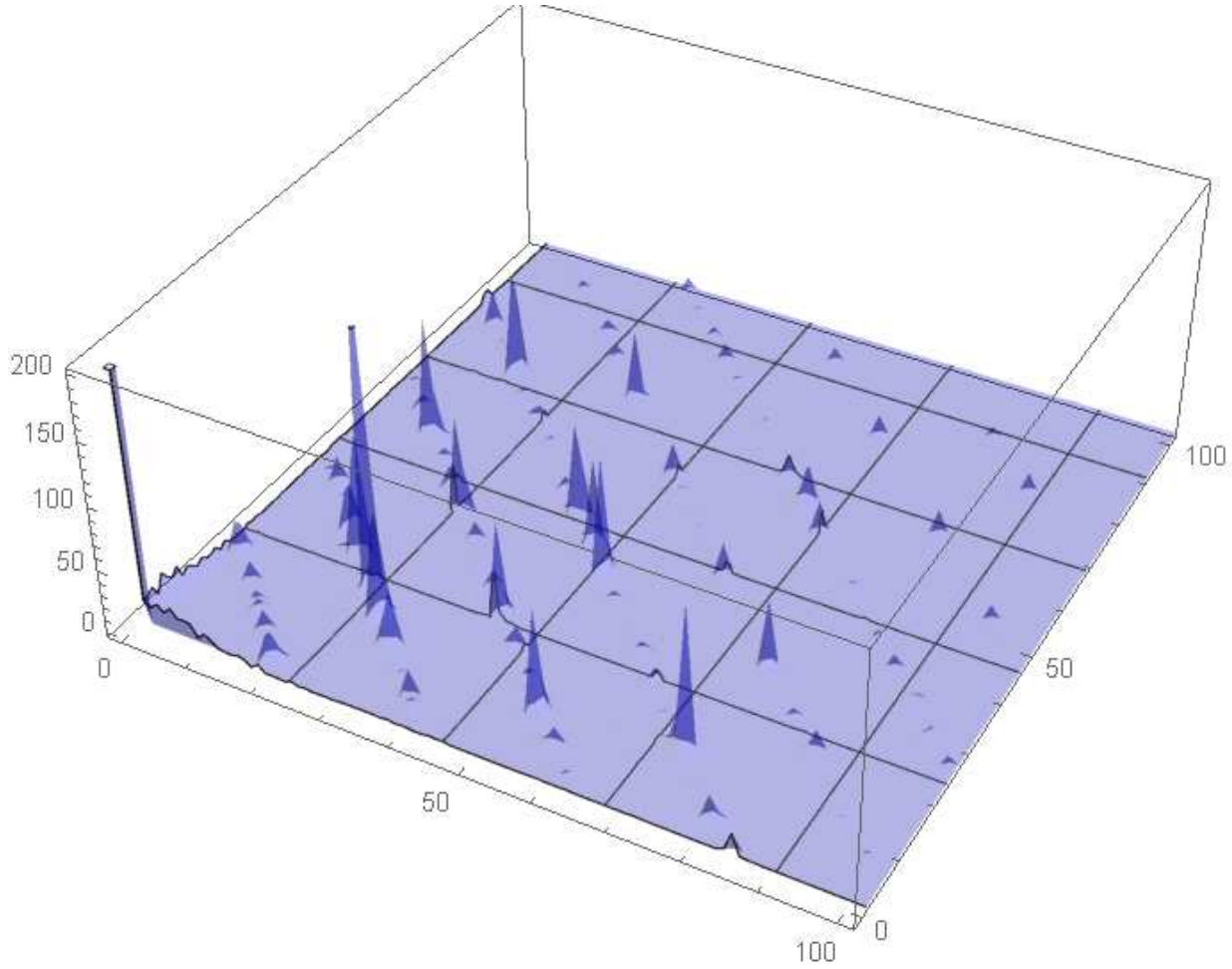

<110>

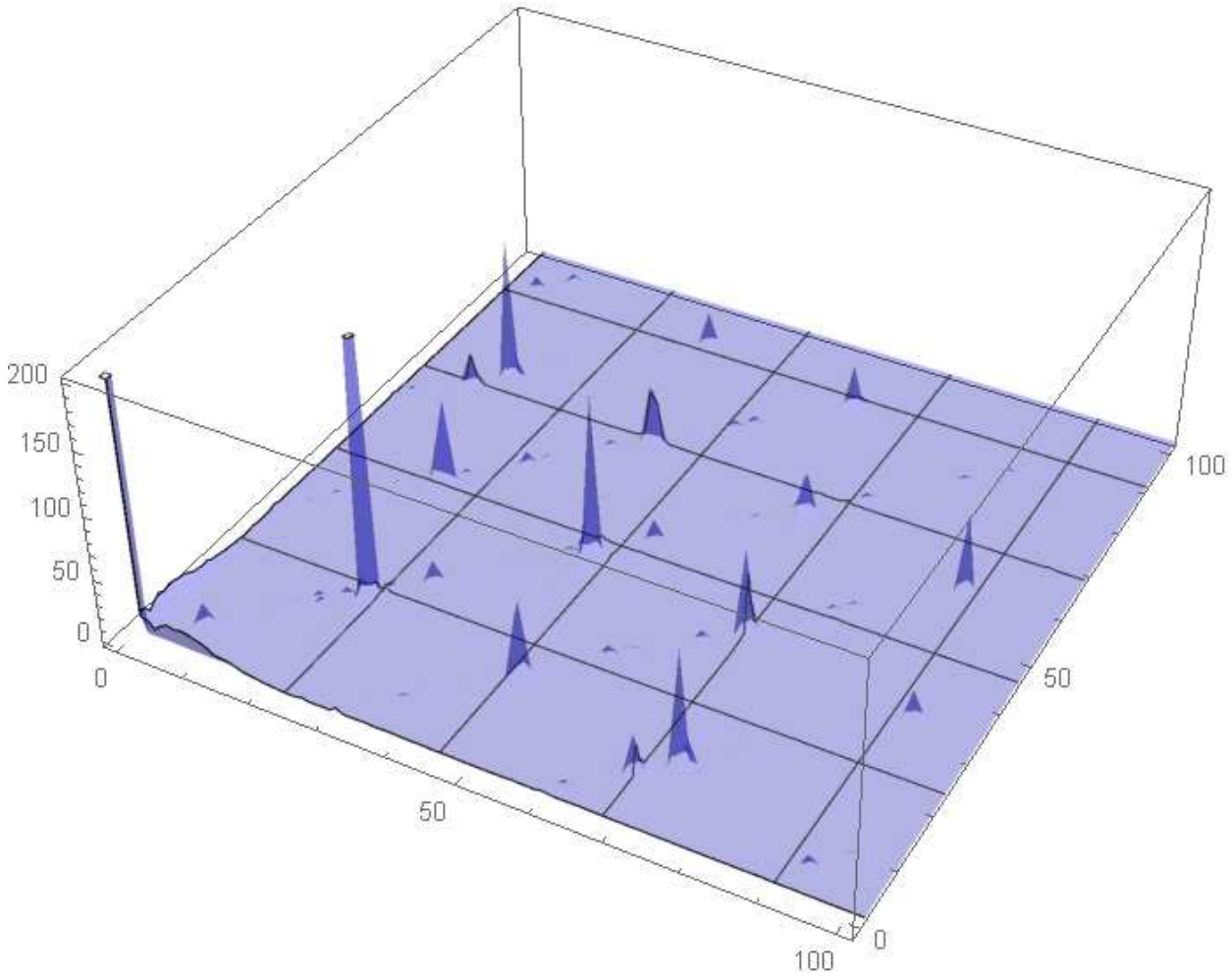

REFERENCES

1. A.S. Joseph, A.C. Thorsen, E. Gertner, and L.E. Valby, Phys. Rev. 148, 569 (1966).
2. N.W. Ashcroft and N.D. Mermin, *Solid State Physics* (Holt, Reiheart and Winston, New York,1976).
3. C. Kittel, *Introduction to Solid State Physics 8-th edition* (John-Wiley & Sons, New York, 2005).
5. D. Shoenberg, Phil. Trans. Roy. Soc. A255, 85-133 (1962).
6. D. Shoenberg, *Magnetic Oscillations in Metal*s (Cambridge, 1984).
7. D.J. Roaf, Phil. Trans. Roy. Soc A255, 135 (1969).
7. M.R. Halse, Phil. Trans. Roy. Soc A265, 507 (1969).
8. F. Han, *A Modern Course in the Quantum Theory of Solids* (World Scientific, 2013).
9. Coleridge and Templeton (1972)
10 S. Altmann, Band Theory of Metals (Pergamon, 1970).

11. J.R. Klauder, W.A. Reed, C.F. Brenner, and J.E. Kunzler, Phys. Rev. 141, 592 (1966).
12. J.M. Ziman, edited, The Physics of Metals1.Electronics (Cambridge, 1969).
13. J.Singleton, Band Theory and Electronic Properties of Solids (Oxford, 2001).

APPENDIX

Mathematica Program: ContourPlot og Cu Fermi surface
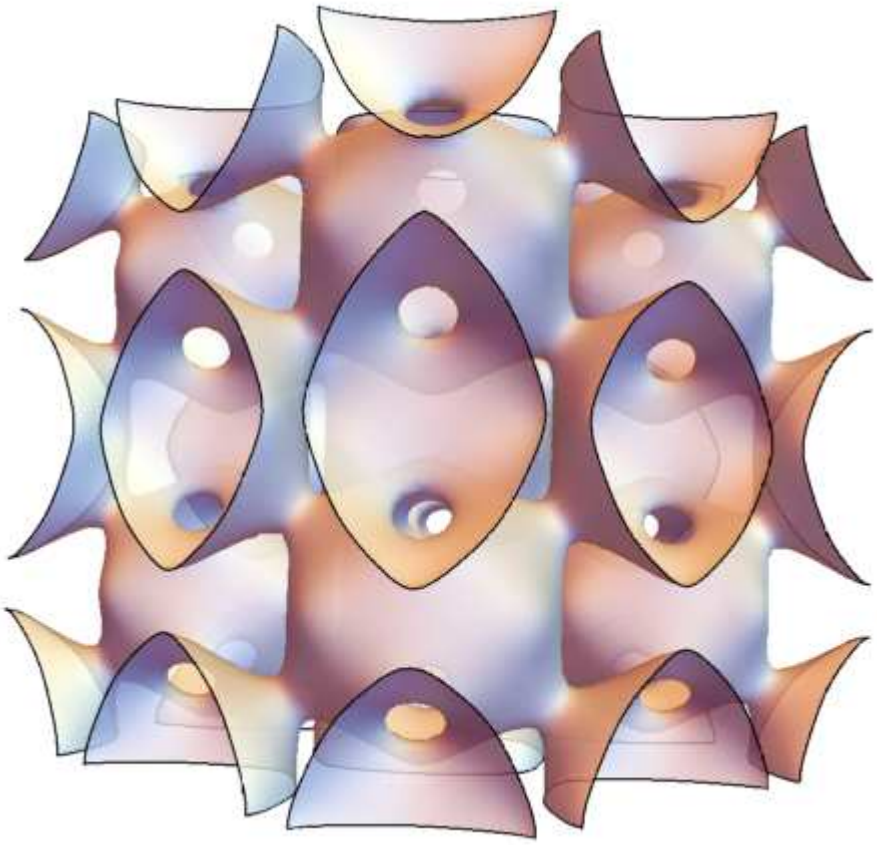
```
Clear["Global`*"];
C0 = 1.691314;
C200 = 0.006574;
C211 = -0.426081;
C220 = -0.018050;
C310 = -0.036283;
C222 = 0;
C321 = 0;
f1 = (3 - Cos[π x] Cos[π y] - Cos[π y] Cos[π z] - Cos[π z] Cos[π x] ) +
  C200 (3 - Cos[2 π x] - Cos[2 π y] - Cos[2 π z]) +
  C211 (3 - Cos[2 π x] Cos[π y] Cos[π z] - Cos[2 π y] Cos[π z] Cos[π x] -
     Cos[2 π z] Cos[π x] Cos[ π y] ) +
  C220 (3 - Cos[2 π x] Cos[2 π y] - Cos[2 π y] Cos[2 π z] -
     Cos[2 π z] Cos[2 π x] ) +
  C310 (6 - Cos[3 π x] Cos[π y] - Cos[3 π y] Cos[π z] - Cos[3 π z] Cos[π x] -
     Cos[3 π y] Cos[π x] - Cos[3 π z] Cos[π y] - Cos[3 π x] Cos[π z]) +
  C222 (1 - Cos[2 π x] Cos[2 π y] Cos[2 π z]) +
  C321 (6 - Cos[3 π x] Cos[2 π y] Cos[π z] - Cos[3 π y] Cos[2 π z] Cos[π x] -
     Cos[3 π z] Cos[2 π x] Cos[π y] - Cos[3 π z] Cos[2 π y] Cos[π x] -
     Cos[3 π x] Cos[2 π z] Cos[π y] - Cos[3 π y] Cos[2 π x] Cos[π z]);
f11 = ContourPlot3D[f1 == C0, {x, -2, 2}, {y, -2, 2}, {z, -2, 2},
  Mesh → None, Axes → False,
  ContourStyle → {Pink, Yellow, White, Opacity[0.8]}, Boxed → False]
```